2017

Open Source Test Bed and Test Case Development for Power System Research

Dheepak Krishnamurthy
Iowa State University

Open source test bed and test case development for power system research

by

Dheepak Krishnamurthy

A thesis submitted to the graduate faculty

in partial fulfillment of the requirements for the degree of

MASTER OF SCIENCE

Major: Electrical Engineering

Program of Study Committee:
Leigh Tesfatsion, Major Professor
James McCalley
Sarah Ryan

The student author and the program of study committee are solely responsible for the content of this thesis. The Graduate College will ensure this thesis is globally accessible and will not permit alterations after a degree is conferred.

Iowa State University

Ames, Iowa

2017

DEDICATION

I would like to thank my major professor Dr. Leigh Tesfatsion without whose support this work would not have been possible. I would like to dedicate this thesis to my friends and family for their encouragement and motivation.

TABLE OF CONTENTS

ABSTRACT

Modeling and simulation of power systems is critical to perform an analysis or study required for industry to adapt and evolve with new technologies. For an analysis or a comprehensive study of a power system, there is a need for a mathematical representation of a model of every element in the power system. For use in an analysis, information and data that pertain to realistic equivalents of parameter being modeled must be attained and employed. Research in academic and scientific studies must also be open, reproducible, and extensible. Replication and reproducability are the cornerstones of the scientific method. Readers of published works must be able to rerun simulations and replicate results, given the information provided in the publication. The results of a published study must also be reproducible using an independent implementation of a method. Open source tools and open source test systems are critical in creating environments where this is possible. For such open, reproducible, and extensible research, two key components are required - open source software and open source data. With open source data, studies can be performed to validate existing models and develop new algorithms using the open source data set as a test benchmark. With Free Open Source Software (FOSS), users are in control to make their own decisions and to do what they want with the software. Users of open source products have access to the source code and debugging tools, and hence often suggest both bug fixes and enhancements as actual changes to the source code. Since the code is open, it's simply a matter of modifying it to add the functionality they want. To use free software is to make a choice asserting the right to learn, and share what we learn with others. Free software has become the foundation of a learning society where we share our knowledge in a way that others can build upon and enjoy. This thesis contributes to open source test system and test bed development in the support of research and engineering for power system optimization, simulation and modeling. It does this in two major ways, described below.

This thesis develops an open-source 8-Zone Test System for teaching, training, and research purposes that is based on ISO New England structural attributes and data. The test system models an ISO-managed wholesale power market populated by a mix of generating companies and load-serving entities that operates through time over an 8-zone transmission grid. The modular extensible architecture of the test system permits a wide range of sensitivity studies to be conducted.

This thesis also further develops AMES with new features in the form of a release as AMES (V4.0). A core component of AMES has been modularized into a separate package called Power System Simulation Toolbox (PSST). PSST includes a power flow, Optimal Power Flow (OPF), wholesale market operation including a Security Constrained Unit Commitment (SCUC) and a Security Constrained Economic Dispatch (SCED). The ease of rapid prototyping and tools provided by this toolkit make this an ideal candidate for power system analysis. Test cases employing these few features are demonstrated to show the value of these capabilities. Additionally, the new features of AMES (V4.0) are thoroughly tested and their performance was characterized.

The main driver for this research is to further develop open source test beds and test systems in support of research and engineering in the power system community. This research aims to further develop an open source test bed and to develop an open source test system for teaching, training, and research purposes. This research also aims to simulate operational aspects of the wholesale electricity markets in an open modular format that is easy to extend by researchers and academia. I have contributed to this effort by releasing an open source eight-zone test system based on ISO-NE data. I have also contributed by improving various features in AMES (Agent-based Modeling of Electricity Systems), an open source wholesale power market simulator. I have also released a tool called power systems simulation toolbox (PSST) that modularizes features of AMES (V4.0) to allow for testing and researching improvements to power system operations simulation.

The research reported in Chapter 1 of this MSc Thesis develops an open-source 8-Zone Test System based on ISO New England structural attributes and data. The test system models an ISO-managed wholesale power market populated by a mix of generating companies and

load-serving entities that operates through time over an 8-zone AC transmission grid. The modular extensible architecture of the test system permits a wide range of sensitivity studies to be conducted. To illustrate the capabilities of the test system, we report energy cost-savings outcomes for a comparative study of stochastic versus deterministic Security Constrained Unit Commitment (SCUC) under systematically varied reserve requirement levels for the deterministic SCUC formulation. This work has been published in the IEEE Transactions on Power Systems [1] with co-authors Wanning Li and Leigh Tesfatsion. Along with my two co-authors, I fully participated in the design of the test system and test case; and I had lead responsibility for all programming and implementation aspects.

The research reported in Chapter 2 descibes improvements to the AMES software and demonstrations of use cases of the new capabilities. This work expands on the previously released AMES (V2.06) [2] to build AMES (V4.0). This work is in collaboration with Auswin Thomas, Sean Mooney and Wanning Li. I was responsible for designing and implementing a Deterministic and Stochastic Security Constrained Unit Commitment and Security Constrained Economic Dispatch in AMES. The implementation was facilitated by Sean Mooney. I was responsible for developing PSST, and integrating it with AMES. PSST is an open source Python package for the simulation of power system operations, and integrates a power flow, Optimal Power Flow (OPF), wholesale market operation including a Security Constrained Unit Commitment (SCUC) and a Security Constrained Economic Dispatch (SCED). This work was published in the North American Power Symposium 2016 [3]. I performed studies such as comparing different formulations using PSST, building a iterative DC-OPF SCUC and ACPF integrated algorithm, and a sensitivity analysis on the number of bid segments in the cost curves of generators. I was also responsible for adding a rolling horizon feature to AMES and for key updates to improve the solution of the optimization.

LIST OF TABLES

LIST OF FIGURES

CHAPTER 1: AN 8-ZONE TEST SYSTEM BASED ON ISO NEW ENGLAND DATA: DEVELOPMENT AND APPLICATION

Published in IEEE Transactions on Power Systems [1]

Dheepak Krishnamurthy, Wanning Li and Leigh Tesfatsion

Abstract

This study develops an open-source 8-zone test system for teaching, training, and research purposes that is based on ISO New England structural attributes and data. The test system models an ISO-managed wholesale power market populated by a mix of generating companies and load-serving entities that operates through time over an 8-zone AC transmission grid. The modular extensible architecture of the test system permits a wide range of sensitivity studies to be conducted. To illustrate the capabilities of the test system, we report energy cost-savings outcomes for a comparative study of stochastic versus deterministic DAM Security Constrained Unit Commitment (SCUC) formulations under systematically varied reserve requirement levels for the deterministic formulation.

1.1 Introduction

1.1.1 General Features of the 8-Zone ISO-NE Test System

The 8-Zone ISO-NE Test System developed in this study, based on structural attributes and data from the New England Independent System Operator (ISO-NE), is an empirically-grounded open-source support tool for power market teaching, training and research. It is a relatively small-scale test system that has been designed to permit the systematic exploratory study of

power market design and performance issues for ISO-NE by means of extensive fast-execution computational experimentation.[1]

Specifically, the test system models a wholesale power market operating through time over an AC transmission grid with congestion managed by locational marginal pricing (LMP). The modeled energy region is divided into eight zones, in accordance with the eight designated load zones for ISO-NE; and generation, load, and transmission line attributes are configured on the basis of current ISO-NE data.

The day-ahead and real-time markets modeled by this test system involve ISO-managed bid/offer-based security-constrained unit commitment (SCUC) and security-constrained economic dispatch (SCED) optimal power flow (OPF) optimizations for the determination of unit commitment, dispatch, and pricing solutions. These solutions are calculated and implemented day after day, where the system state at the beginning of each day D is determined as a function of the previous state at the beginning of day D-1 together with internal system events and external environmental events occurring during day D-1.

This dynamic state-space modeling approach permits the study of both market efficiency and system reliability over time. For example, the effects of a change in a market operating procedure on the welfare (profits and losses) of market participants, and on the stability of system operations as a whole, can be studied over the short, intermediate, and long run, taking into account the responses of market participants and system conditions to this change.

Although the 8-Zone ISO-NE Test System is configured using structural attributes and data from ISO-NE, it is implemented by means of the AMES Wholesale Power Market Test Bed [2], a Java/Python package of classes with a modular and extensible architecture. Consequently, users of the test system can easily modify its features to match the operations of other wholesale power markets, or to model and study proposed market design elements that have not yet been implemented. For example, the test system's Graphical User Interface (GUI) permits users to vary the generation mix for their own purposes by introducing generation units with distinct

[1] DOE's Technology Readiness Levels [4] range from TRL 1 (initial conceptual development) to TRL 9 (commercial application). Under the DOE ARPA-E project that funded this study's research, with ISO-NE as a participating partner, the 8-Zone ISO-NE Test System was deliberately designed as a TRL 4 test system to help bridge the "valley of death" (TRLs 4-6) that must be crossed in order to bring typical university research (TRLs 1-3) into contact with typical industry research (TRLs 7-9).

names, locations, fuel types, capacities, start-up costs, no-load costs, dispatch cost coefficients, and ramping capabilities.

1.1.2 Comparison with Previously Developed Test Systems

The 8-Zone ISO-NE Test System differs in purpose, availability, and scale from previously developed test systems for power system analysis.

Some researchers in collaboration with industry partners have been able to make use of ISO/RTO-scale systems; see, for example, [5]. However, these systems are not open source and are not easy to access for most researchers. Moreover, the systems are so large and complex that it is difficult to use them for intensive sensitivity studies.

Other researchers have developed publicly available test systems; but, to date, these systems have largely been designed to facilitate the study of system stability at relatively small time scales rather than the study of market performance over successive days. Examples include the IEEE reliability test systems stored at the University of Washington archive ([6],[7]) as well as more recently developed test systems such as [8] and [9]. For example, in [9] a power flow study is conducted for a 68-bus system to determine initial steady-state values, and state-space matrices and eigenvalues are then determined for the linearized system at this initial point in order to enable a study of local system stability.

The traditional IEEE benchmark-system focus on power flow problems for local stability analysis has been extended in more recent test systems and software packages to permit a consideration of OPF solutions based on the bids and offers of market participants. This development reflects the increasing use of OPF optimizations in centrally-managed wholesale power markets.

For example, MATPOWER [10] is a package of Matlab M-files designed for solving both power flow and OPF problems. Nevertheless, the focus of MATPOWER is still on stability issues arising at relatively small time scales. Moreover, although top-level MATPOWER code is now being distributed under a GNU General Public License (GPL), MATPOWER is based on Matlab for which core aspects are proprietary; hence, exceptions are included in the GPL to ensure proprietary Matlab code is protected.

In recent years a number of researchers have attempted to redress the relative lack of publicly available market-oriented test systems. For example, variants of a 5-bus test system originally developed in 2002 by John Lally [11, Section 6] for the study of the financial transmission rights market in ISO-NE are now being used for more general market training by ISO-NE, PJM, and other ISO/RTO-managed U.S. energy regions.

As detailed in Sun and Tesfatsion [12] and Li and Tesfatsion [13], the Lally 5-bus test system has been developed into a more fully articulated 5-Bus Test Case included (along with a 2-Bus Test Case and a 30-Bus Test Case) in the open-source release of the AMES Wholesale Power Market Test Bed [2]. In addition, Li and Bo [14] have suggested various ways to improve a version of the Lally 5-bus test system in use by PJM, such as the introduction of differentiated loads across the three load buses for increased clarity. Li and Bo also discuss a number of modifications proposed by themselves and others for the IEEE 30-bus reliability test system that would increase its usefulness for market study purposes.

In contrast to the 8-Zone ISO-NE Test System, however, the specification of structural attributes and parameter values for these previously developed small-scale market-oriented test systems are largely arbitrary, for illustrative purposes only. No attempt has been made to base these specifications on the empirical conditions of an actual energy region.

The 8-Zone ISO-NE Test System also differs in purpose from larger-scale market-oriented test systems, such as the FERC test system [15] and the WECC test system [16]. These test systems have been designed for commercial-grade application, not for exploratory fast-execution simulation studies. The FERC test system provides a large-scale PJM-based data set and unit commitment (UC) formulation to facilitate the comparative study of alternative DAM and residual UC solvers. The 240-bus WECC test system provides a realistic large-scale test system for the California Independent System Operator (CAISO) and the Western Electricity Coordination Council (WECC) for the purpose of studying possible improvements to existing market features.

1.1.3 Motivation for the Illustrative Application

The recent rapid growth of variable generation, resulting in increased supply uncertainty, has encouraged efforts to develop improved stochastic security-constrained unit commitment (SCUC) optimization tools. See, for example, Morales et al. [17], Papavasiliou et al. [18], and Vrakopoulou et al. [19].

To illustrate the capabilities of the 8-Zone ISO-NE Test System, we report on its use for a comparative study of stochastic versus deterministic DAM SCUC formulations under varied reserve requirement levels for the deterministic formulation.[2] In contrast to previous comparative SCUC studies (e.g., [18]), performance is measured in terms of energy cost saving taking into account both day-ahead unit commitment costs and real-time dispatch costs.

Also, a detailed analysis is undertaken to understand the reasons for observed performance differences. Specifically, the reported results reveal the critical roles played by scenario specification bias, load dispersion, generation mix, and reserve requirements in determining the extent to which a switch from a deterministic to a stochastic DAM SCUC formulation results in energy cost savings.

1.1.4 Study Organization

The remainder of this study is organized as follows. Section 1.2 discusses the computational platform (AMES) used to implement the 8-Zone ISO-NE Test System. Section 1.3 describes the basic components of the test system. An illustrative application of this test system, a comparison of stochastic vs. deterministic DAM SCUC formulations, is discussed in Section 1.4, and key findings from this illustrative application are reported in Section 1.5. Concluding remarks are given in 1.6.

Finally, a detailed mathematical presentation of the stochastic DAM SCUC formulation for our illustrative application is provided in an appendix, together with a nomenclature table.

[2] As will be clarified in Section 1.4, it is commonly assumed for stochastic SCUC optimizations that the set of scenarios specified for possible future load realizations covers all possible uncertainties, and that power-balance constraints are scenario-conditioned. Consequently, reserve-requirement constraints are not considered. In practice, it might of course be prudent to continue to impose reserve-requirement constraints to insure against the possibility that the specified scenario set does not in fact provide complete coverage of uncertainties.

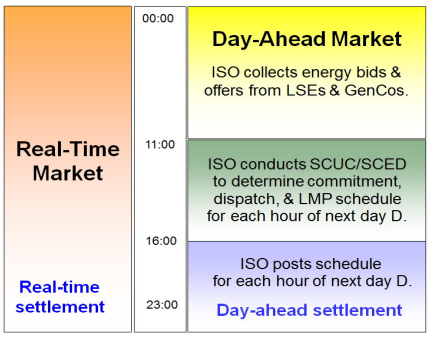

Figure 1.1: Two-settlement market design: ISO activities on a typical day D-1

Complete Java/Python code files and data files for the 8-Zone ISO-NE Test System are provided at [20].

1.2 Implementation via the AMES Test Bed

In a 2003 report [21] the U.S. Federal Energy Regulatory Commission (FERC) proposed the adoption of a market design for improved wholesale power system operations. This design has since been implemented in seven U.S. energy regions encompassing over 60% of U.S. generation capacity. The core feature of this design is a two-settlement system, centrally managed by an independent system operator (ISO) or regional transmission organization (RTO).

As depicted in Fig. 1.1, this two-settlement system consists of a daily day-ahead market (DAM) for the commitment and scheduling of generation for next-day operations and a daily 24-hour real-time market (RTM) functioning as a balancing mechanism to handle any residual load-balancing needs. In both markets, transmission congestion is managed by locational marginal pricing (LMP).

AMES (Agent-based Modeling of Electricity Systems) [2] is an agent-based Java/Python computational platform permitting the systematic study of dynamic wholesale power systems structured in accordance with FERC's two-settlement market design. The 8-Zone ISO-NE Test System developed in this study is implemented by means of AMES (V4.0).

As depicted in Fig. 1.2, AMES (V4.0) models an ISO-managed wholesale power market operating during time-periods $k = 1, 2, \ldots$, over an AC transmission grid. Participants in this

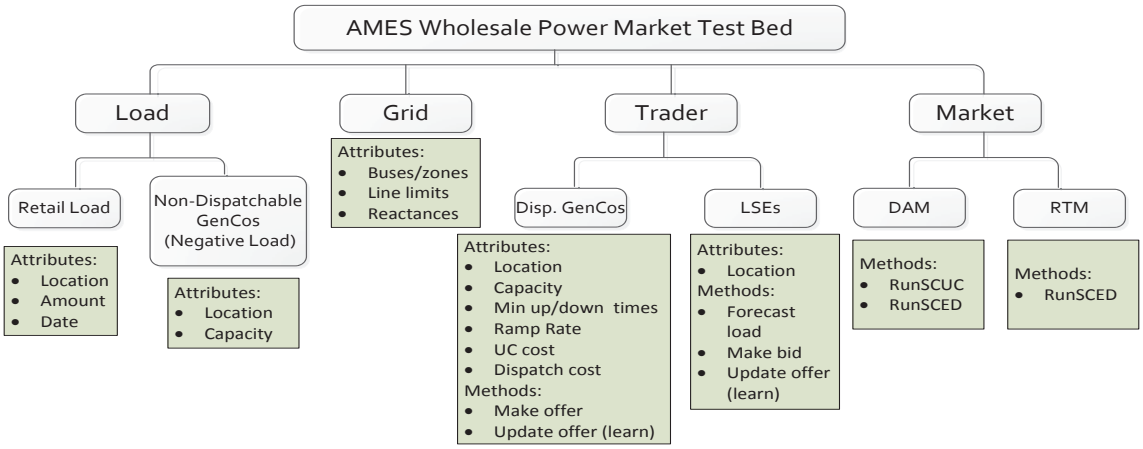

Figure 1.2: Key components of AMES (V4.0)

market include Generation Companies (GenCos) as well as Load-Serving Entities (LSEs) servicing the energy needs of retail customers. The GenCos can include generators (e.g., thermal) with dispatchable power as well as generators (e.g., solar, wind) with non-dispatchable power treated as negative load.

The dispatchable GenCos submit supply offers into the DAM and the RTM consisting of fixed and/or price-responsive portions. The LSEs submit demand bids into the DAM consisting of fixed and/or price-responsive portions. AMES (V4.0) includes a learning module that permits GenCos and/or LSEs to be modeled as learning agents capable of changing their offer/bid methods over time on the basis of past experiences.

In the DAM, the ISO conducts bid/offer-based SCUC and bid/offer-based SCED optimizations to determine the commitment and scheduled dispatch of generation to meet forecasted next-day loads, as determined from LSE demand bids. In the RTM, the ISO conducts an offer-based SCED optimization to resolve imbalances between DAM-scheduled generation and ISO forecasted real-time loads. A cost for curtailed load is included in the SCUC/SCED objective functions as a summation of power-balance slack terms multiplied by a user-specified penalty weight.

Dispatchable GenCos in AMES (V4.0) can incur both UC and dispatch costs, where the UC costs take the form of start-up, no-load, and shut-down costs. The performance metric

considered in later sections of this study is cost saving, where cost consists of both UC costs and dispatch costs measured in terms of energy usage.[3] Consequently, it is important to understand the precise distinctions among these various types of costs.

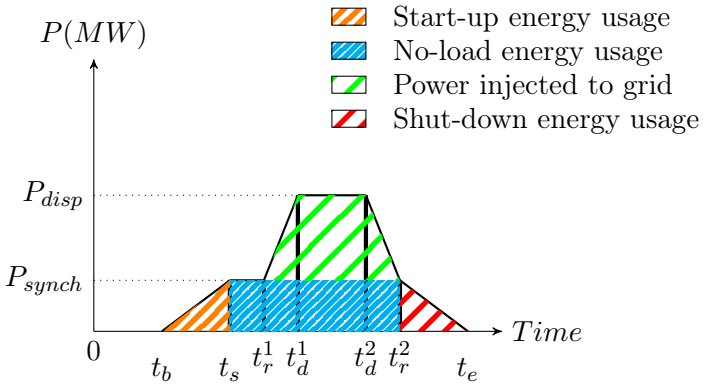

Figure 1.3: Energy usage over time for a generation unit

Figure 1.3 illustrates the various ways that a generator can use energy as a result of commitment and dispatch, and hence incur UC and dispatch costs. In Fig. 1.3, a dispatchable generator g in a shut-down condition at time 0 is scheduled to inject power into the grid at level $P = [P_{\text{disp}} - P_{\text{synch}}]$ during time interval $[t_d^1, t_d^2]$. During the time interval $[t_b, t_s]$, g ramps up to the power level P_{synch} at which it is spinning at synchronous speed, ready to inject power into the grid. During the time interval $[t_s, t_r^1]$, g remains in a synchronized state with no injection of power into the grid. During time interval $[t_r^1, t_d^1]$, g ramps up to reach the power level P_{disp}; and g maintains this power level over the time interval $[t_d^1, t_d^2]$. At time t_d^2 generator g initiates a ramp-down process. During the initial ramp-down stage $[t_d^2, t_r^2]$, g is still injecting power into the grid. At time t_r^2, g reaches the power level P_{synch} at which it is synchronized to the grid but not injecting power into the grid. Generator g then continues to ramp down until it reaches a shut-down state at time t_e.

The costs of the energy used by g over the time interval $[t_b, t_s]$ to attain a synchronized state, starting from a shut-down state, are called *start-up costs*. The costs of the energy used by g to remain synchronized during the time interval $[t_s, t_r^2]$ are called *no-load costs*. The costs

[3] UC costs can also include non-energy related costs, such as the wear and tear on machinery from the start-up, shut-down, and/or synchronized running of generation units. In AMES (V4.0) only energy costs are considered.

of the energy injected by g into the grid during the scheduled dispatch interval $[t_d^1, t_d^2]$ are called *dispatch costs*.[4] Finally, the costs of the energy used by g over the time interval $[t_r^2, t_e]$ to attain a shut-down state, starting from a synchronized state, are called *shut-down costs*.

AMES (V4.0) calculates dispatch and start-up/shut-down costs by dispatch and start-up/shut-down energy usage, as depicted in Fig. 1.3. However, no-load costs are calculated only for the duration of time during which a generator is dispatched. That is, the presumption is that a committed generator can time its synchronization point to coincide with the start of its dispatch period so that no-load energy usage as depicted by the energy block t_s-t_r^1-P_{synch} in Fig. 1.3 does not arise.

1.3 The 8-Zone ISO-NE Test System

This section discusses our construction and benchmark configuration of the 8-Zone ISO-NE Test System based on ISO-NE structural attributes and data.[5] Detailed code and benchmark data configuration files for the test system can be obtained at the repository site [20]. A user can either keep our benchmark settings or change them to user-specified values via the test system's graphical user interface (GUI).

1.3.1 Transmission Grid

ISO-NE is part of the Northeast Power Coordinating Council (NPCC) reliability region. The states covered by ISO-NE are Connecticut, Maine, Massachusetts, New Hampshire, Rhode Island and Vermont. The ISO-NE energy region is divided into eight load zones: namely, Connecticut (CT), Maine (ME), New Hampshire (NH), Rhode Island (RI), Vermont (VT), Northeastern Massachusetts/Boston (NEMA/BOST), Southeastern Massachusetts (SEMA) and Western/Central Massachusetts (WCMA) [22].

[4] In current U.S. DAM operations, generators are typically not compensated for the energy they expend in ramping from a syncronized state to a scheduled dispatch level that is about to start or back to a synchronized state from a scheduled dispatch level that has just concluded.

[5] Some data were directly supplied to us by ISO-NE, a participating partner in the ARPA-E project that supported our research. However, these data were incomplete in some regards for our market analysis purposes. As clarified below, the needed missing data were obtained from other reliable sources.

To reflect this configuration, our 8-Zone ISO-NE Test System consists of eight zones connected by an AC transmission grid consisting of twelve transmission lines; see Fig. 1.4. Flows with neighboring energy regions are not considered. Since transmission projects placed in service in ISO-NE over the past decade have substantially reduced congestion, the benchmark capacity (power limit) of each line in the 12-line test-system grid is set at a relatively high level.

The resistance and reactance benchmark values for the 12-line test-system grid are set based on physical considerations. The key factors that determine these values include the length of each line, conductor type, conductor bundling and transposition, and temperature. Each line is assumed to be a single-circuit 345kV AC line with a 6-conductor bundle per phase, using conductor type Dove (556 kcmil). The bundles have $2.5'$ diameter and the phases are separated by $45'$. The temperature is assumed to be constant at 25 degrees Celsius. Given these physical attributes, resistance and reactance values (per unit of length) are derived from ACSR cable parameter tables for overhead transmission lines: namely, Table A8.1 in [23] and Tables 3.3.1-3.3.13 in [24].

The length of each line in our 12-line test-system grid is measured by the distance between the two ISO-NE zones that it connects, where each zone is represented as a point located at a central city within the zone. The benchmark resistance and reactance values for each line are then obtained by multiplying the resistance and reactance values (per unit of length) by the line length; see Table 1.1. In the last column of Table 1.1, reactance (ohms) is converted into per unit (pu) using 345kV as the base voltage value and 100MVA as the base volt-ampere value.

Table 1.1: Resistance and Reactance Benchmark Values for the 8-Zone ISO-NE Test System

Line	From Zone	To Zone	Distance (miles)	Resistance (ohms)	Reactance (ohms)	Reactance (per unit)
1	ME	NH	115.00	19.09	54.05	0.05
2	VT	NH	100.00	16.60	47.00	0.04
3	VT	WCMA	150.00	24.90	70.50	0.06
4	WCMA	NH	86.00	14.28	40.42	0.03
5	NEMA/BOST	WCMA	80.00	13.28	37.60	0.03
6	NEMA/BOST	NH	63.00	10.46	29.61	0.02
7	NEMA/BOST	SEMA	30.00	4.98	14.10	0.01
8	WCMA	CT	30.00	4.98	14.10	0.01
9	WCMA	RI	65.00	10.79	30.55	0.03
10	NEMA/BOST	RI	40.00	6.64	18.80	0.02
11	CT	RI	64.00	10.62	30.08	0.03
12	SEMA	RI	20.00	3.32	9.40	0.01

1.3.2 Generator Attributes

As detailed in [25], the generation mix for ISO-NE currently consists of 436 generation units with a total installed capacity of 32,000MW. Roughly 88% of this capacity is provided by 151 thermal generation units. The remaining 12% is provided by generation units consisting of traditional hydro (4%), pumped hydroelectric storage (5%), and other renewables (3%). The latter category includes 73 wind farms (2.5%), generally small in size.

To obtain a benchmark generation mix for our 8-Zone ISO-NE Test System, this actual ISO-NE generation mix was reduced in size as follows. First, all non-thermal generation units were

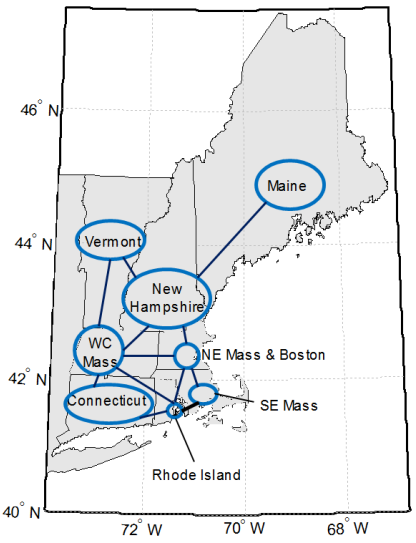

Figure 1.4: Transmission grid for the 8-Zone ISO-NE Test System

removed. This was done to avoid having to undertake relatively complicated special modeling for only a small portion of total installed generation capacity.[6]

Second, 76 of the remaining 151 thermal generation units were selected for inclusion in the benchmark generation mix, each treated as an independent generator. These 76 generators have a combined installed generation capacity of 23,100MW and account for 72% of the actual ISO-NE capacity (32,000MW). As indicated in Fig. 1.5, in implementing this selection, care was taken to ensure that the overall proportions of thermal generation (by fuel type) for the test system roughly match the overall proportions of thermal generation (by fuel type) in ISO-NE. In addition, care was taken to ensure that the proportions of thermal generation (by fuel type) specified for each of the eight zones in the test system roughly match the actual proportions of thermal generation (by fuel type) in each of the eight corresponding ISO-NE load zones.

[6]The modeling of hydro units is relatively complicated, requiring water resource planning and optimization techniques involving considerations of water supply, reservoir management, and flood control. This modeling is further complicated by the need to consider seasonal and cyclic variability of stochastic quantities such as reservoir inflows. Furthermore, these types of generation units often resort to self-scheduling of their generation offers in the DAM, hence there is only limited information on their offer methods. Similarly, the inclusion of wind generation would require a careful modeling of the special treatment of wind generation in the ISO-NE, including the extent to which the ISO-NE permits wind generation to be offered into the DAM, the extent to which the ISO-NE is able to use wind spillage as reg down, and the manner in which sudden strong ramp events caused by wind penetration are handled. However, as noted in Section 1.2, our test system is implemented by means of the modular and extensible AMES (V4.0) test bed. This should facilitate the inclusion of hydro, wind, and other renewable generation sources in future extensions of our test system.

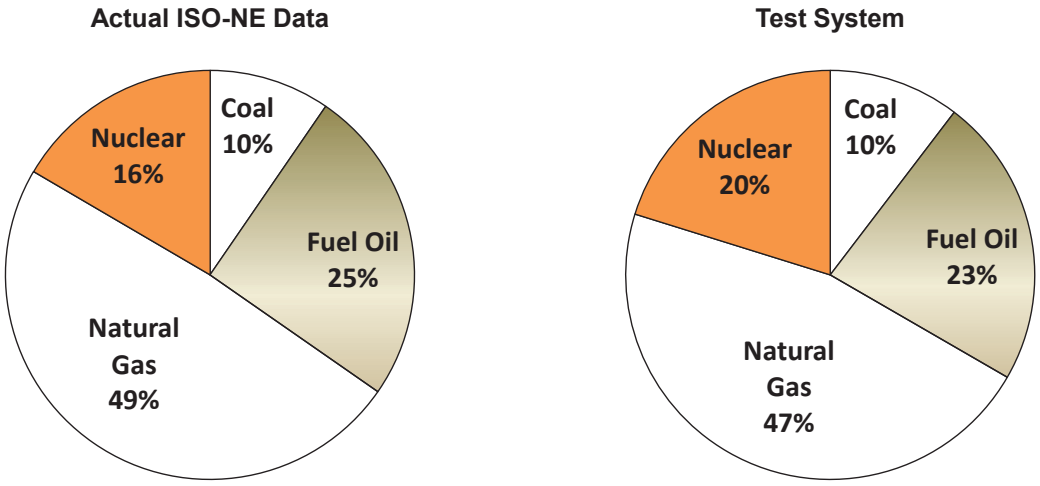

Figure 1.5: Comparison of ISO-NE and 8-Zone ISO-NE Test System thermal generation capacity proportions by fuel type

The 76 benchmark thermal generators for the 8-Zone ISO-NE Test System incur both UC costs and dispatch costs, where the UC costs include start-up, no-load, and shut-down costs. Additional generator attributes in need of specification include ramp rates and minimum up/-down times.

The MBtu per start for a generator is classified as hot or cold, depending on the time that the generator has been offline. These hot/cold values can differ, and they depend on the generator's fuel type and capacity. The hot/cold MBtu per start for a generator multiplied by the cost per MBtu for that generator's fuel type gives the generator's hot/cold start-up costs. Similarly, the MBtu per stop for a generator multiplied by the cost per MBtu for that generator's fuel type gives the generator's shut-down costs. Data on hot/cold MBtu/start and MBtu/stop for different fuel types and capacities were obtained from the provided ISO-NE data. The costs per MBtu for generators with different fuel types were obtained from the U.S. Energy Information Administration (EIA) [26].

The no-load cost for each of the benchmark thermal generators by fuel type and capacity was derived from the detailed data provided in [27] for ISO-NE energy offer data. A summary indication of these no-load costs by fuel type and capacity range is given in Table 1.2.

Table 1.2: No-load costs by fuel type and capacity.

Fuel type	Capacity (MW)	No-load cost ($/hr)
Coal	0 – 75	236 – 238
Coal	75 – 150	238 – 745
Coal	150 – 350	745 – 1213
Coal	$>$ 350	1213 – 3043
Fuel Oil	0 – 80	0 – 1500
Fuel Oil	80 – 200	1500 – 2000
Fuel Oil	200 – 400	2000 – 3500
Fuel Oil	400 – 600	3500 – 10379
Natural Gas	0 – 400	0 – 600
Natural Gas	400 – 600	600 – 3859
Nuclear	–	1000 – 1500

The total dispatch cost function ($/h) for each benchmark generator g in each hour k is assumed to take the following form:

$$C_{P,g} = a_g p_g + b_g [p_g]^2 \tag{1.1}$$

where p_g (MW) denotes g's power output. Benchmark settings for the cost coefficients a_g and b_g in (1.1) were derived from ISO-NE generation block-offer schedule data differentiated by fuel type [27]. A summary indication of these benchmark cost-coefficient settings by fuel type is given in Table 1.3.

Table 1.3: Dispatch cost coefficients by fuel type.

Fuel type	a ($/MWh)	b ($/MW^{2}h)
Coal (BIT)	18.28	0.000116
Coal (SUB)	19.98	0.001667
Fuel Oil	150 – 233	0.0059 – 0.0342
Natural Gas	23.13 – 57.03	0.002 – 0.008
Nuclear	5-11	0.00015 – 0.00023

A generator's ramp rate (MW/min) is the amount by which the generator can ramp its power output up or down in one minute. Ramp rates by fuel type, provided in [28], are displayed in Table 1.4. These ramp rates were used to configure the ramp rates for the benchmark generators. Finally, minimum up/down times for the benchmark generators were fully specified on the basis of provided ISO-NE data.

Table 1.4: Ramp rates by fuel type.

Fuel Type	Ramp Rate MW/min
Coal	2.0
Fuel Oil	2.0
Natural Gas	6.7
Nuclear	2.0

Complete attribute specifications for each of the 76 benchmark generators for the 8-Zone ISO-NE Test System are provided at the repository site [20]. As indicated above, these specifications include zone location, fuel type, capacity, start-up costs, no-load costs, shut-down costs, dispatch cost coefficients, ramp rates, and minimum up/down times.

1.3.3 LSE Attributes

The 8-Zone ISO-NE Test System has eight zones z, each serviced by a single aggregate load-serving entity LSE_z. Specifically, LSE_z submits a demand bid into the DAM on each day D-1 that takes the form of a forecasted 24-hour zone-z load profile for day D.[7]

As will be clarified in Section 1.4.3, the load scenarios used in the illustrative application of the 8-Zone ISO-NE Test System are based on actual ISO-NE load data; and LSE load forecasts take the form of load expectations (probability-weighted averages) calculated on the basis of these load scenarios.

1.3.4 Reserve Requirements

The 8-Zone ISO-NE Test System permits the inclusion of user-specified zonal and system-wide reserve requirements in the day-ahead and/or real-time SCUC/SCED optimizations. Reserve in the 8-Zone ISO-NE Test System consists of the unencumbered (non-dispatched) capacity of the DAM-committed generators.[8] System-wide reserve consists of the unencumbered capacity of all committed generators, regardless of their location. Zonal reserve for a particular zone z consists of the unencumbered capacity of all committed generators located in zone z.

1.4 Illustrative Application: Overview

1.4.1 Purpose and General Scope

To illustrate the capabilities of the 8-Zone ISO-NE Test System, we have used the test system to conduct a comparative study of stochastic versus deterministic DAM SCUC formulations. For simplicity of exposition, this illustrative application assumes: (i) the only source of uncertainty at the time of the DAM is possible next-day load-profile realizations; (ii) the power limits for the

[7] To date, the vast majority of loads in ISO-NE are not directly responsive to wholesale prices, and the current construction of the 8-Zone ISO-NE Test System reflects this reality. However, AMES (V4.0) permits LSE demand bids to be price responsive, hence the 8-Zone ISO-NE Test System could easily permit this as well.

[8] In actual ISO-NE operations, the commitment of generators with low UC costs and high dispatch costs can be delayed until later residual unit commitment processes, called Reserve Adequacy Analysis (RAA) processes in ISO-NE, if these generators are quick-start fast-ramp units. Currently our test system only includes a DAM SCUC/SCED and an RTM SCED; it does not include RAA processes. Consequently, we include all generators in the DAM to approximate the total commitment that would occur with both a DAM and a subsequent RAA process.

12-line test-system grid are set high enough to ensure that no transmission congestion occurs; and (iii) the deterministic DAM SCUC formulation includes a system-wide reserve-requirement constraint but no zonal reserve constraints.

Attention is focused on the degree to which a switch from a deterministic to a stochastic DAM SCUC formulation would result in cost saving under variously specified reserve-requirement levels for the deterministic formulation. For the stochastic formulation, the ISO conditions its optimization on a set $\mathcal{S}$ of scenarios for possible future load realizations, together with associated scenario probabilities. For the deterministic formulation, the ISO conditions its optimization on an *expected* future load realization calculated on the basis of these same scenarios and probabilities.[9]

To illustrate how our test system can be used to test the robustness of alternative DAM SCUC formulations against errors in the ISO's modeling of uncertain loads, we assume the ISO's anticipated load-scenario set $\mathcal{S}$ contains only five load scenarios when, in actuality, ten load scenarios are possible.

1.4.2 Stochastic vs. Deterministic DAM SCUC Formulations

Our stochastic DAM SCUC formulation is based on the well-known deterministic SCUC formulation developed by Carrion and Arroyo [29]. We extended the Carrion/Arroyo formulation to a two-stage stochastic DAM SCUC formulation. The complete structural form of this stochastic DAM SCUC formulation is provided in an appendix, together with a nomenclature table. Here we give a summary outline of this formulation.

The objective of the ISO in our stochastic DAM SCUC formulation is to minimize expected total energy cost subject to system and UC constraints, where expectations are taken with respect to a set $\mathcal{S}$ of scenarios for possible future loads. As will be explained in Section 1.4.3, the scenarios in $\mathcal{S}$ are mean-zero perturbations of LSE demand bids.

[9] As will be clarified below, the expectation for each zone-conditioned scenario in the ISO's anticipated load-scenario set $\mathcal{S}$ coincides, by construction, with the corresponding zonal load-profile forecast implied by DAM LSE demand bids. In actual ISO-NE deterministic DAM SCUC operations, the ISO is required to use LSE demand bids as its forecasted next-day loads.

Expected total energy cost is then the summation of *first-stage costs* (i.e., DAM UC costs) plus the expected level of *second-stage costs* (i.e., real-time dispatch costs plus penalty costs imposed for any real-time load curtailment). Using nomenclature defined in the appendix, expected total energy cost in analytical form is given by

$$\sum_{k\in K}\sum_{g\in\mathcal{G}}[C_{U,g}(k)+C_{N,g}(k)+C_{D,g}(k)] \\ +\sum_{s\in S}\pi^s\sum_{k\in K}\sum_{g\in\mathcal{G}}C^s_{P,g}(k)+\Lambda\sum_{s\in S}\pi^s\sum_{z\in\mathcal{Z}}\sum_{k\in K}\gamma^s(z,k) \tag{1.2}$$

The decision variables for our stochastic DAM SCUC formulation are classified as follows:

- First-stage decision variables: Generator on/off commitment indicator variables, not scenario-conditioned
- Second-stage decision variables: Scenario-conditioned generator dispatch and voltage angle levels

The key types of system and UC constraints are as follows:

- Scenario-conditioned power balance constraints (by zone)
- Scenario-conditioned generation capacity constraints
- Scenario-conditioned transmission line constraints
- Scenario-conditioned ramp constraints
- Start-up/shut-down constraints
- Minimum up/down time constraints

Our deterministic DAM SCUC formulation is derived from our stochastic DAM SCUC formulation as follows. We first consider the reduced form of our stochastic DAM SCUC formulation obtained by considering only one load scenario $\bar{s}$, calculated as the expectation (probability-weighted average) of the load scenarios in the scenario set $\mathcal{S}$ for the stochastic

case. The objective function for this deterministic DAM SCUC formulation thus takes the following form:

$$\sum_{k\in K}\sum_{g\in\mathcal{G}}\left[C_{U,g}(k)+C_{N,g}(k)+C_{D,g}(k)+C^{\bar{s}}_{P,g}(k)\right]$$
$$+\Lambda\sum_{z\in\mathcal{Z}}\sum_{k\in K}\gamma^{\bar{s}}(z,k) \tag{1.3}$$

We next augment the constraints for this reduced single-scenario DAM SCUC formulation with system-wide reserve-requirement (RR) constraints of the form

$$\sum_{g\in\mathcal{G}}\overline{p}^{\bar{s}}_{g}(k)\geq\sum_{z\in\mathcal{Z}}L^{\bar{s}}(z,k)+RR(k) \tag{1.4}$$

for each hour $k\in K$, where: $\overline{p}^{\bar{s}}_{g}(k)$ (MW) denotes the maximum available power output of generator g in hour k, given scenario $\bar{s}$; $L^{\bar{s}}(z,k)$ (MW) denotes the ISO's forecasted load for zone z in hour k, given scenario $\bar{s}$; and $RR(k)$ (MW) denotes the system-wide reserve requirement for hour k.

1.4.3 Construction of Load Scenarios and LSE Demand Bids

The load scenarios for our illustrative application are two-day scenarios based on scaled[10] ISO-NE March hourly load data for 2004-2006, separately reported for each of ISO-NE's eight load zones.[11]

Using these data, we first generated 90 two-day hourly load scenarios, where each load scenario consisted of eight zone-conditional components. Each of these 90 scenarios was assigned an equal probability of 1/90.

We next used a well-known scenario reduction method [30] based on similarity clustering to reduce these original 90 load scenarios to a smaller collection $\mathcal{S}$ containing five load scenarios of the form $s=(s(z_1),\ldots,s(z_8))$, where s_z denotes a two-day hourly load scenario for zone z.

[10] As detailed in Section 1.3.2, the benchmark generation mix for our 8-Zone ISO-NE Test System is a scaled-down representation of the actual ISO-NE generation mix that captures 72% of actual ISO-NE total installed generation capacity. For consistency, we scale the load data for our illustrative application to 72% of actual ISO-NE loads.

[11] As detailed in Section1.4.4, our illustrative application uses two-day load scenarios to conduct two-day simulations. However, expected cost saving is only reported for the second day since first-day results can be distorted by initial conditions. Additional important but technical implementation details are discussed at the test system code and data repository site [20].

Each $s \in \mathcal{S}$ was then assigned a probability π^s equal to the sum of the probabilities for the original load scenarios lying in its cluster.

The elements $s \in \mathcal{S}$ are assumed to be the load scenarios that the ISO anticipates could be realized for zones $z_1, \ldots, z_8$ over days D and D+1 from the vantage point of the current DAM on day D-1. For each zone z, the demand bids submitted by LSE_z into the DAM on days D-1 and D for its retail zone-z customers on days D and D+1 are constructed to coincide with the expectation (probability-weighted average) of the elements $\{s(z) \mid s \in \mathcal{S}\}$. This construction can be given the following as-if interpretation: The ISO treats DAM LSE demand bids as unbiased forecasts for future loads and specifies possible future load scenarios as mean-zero perturbations about these unbiased forecasts.

In reality, ISOs cannot specify scenario sets that correctly and completely represent all possible future load realizations. Consequently, it is important to study how biases in an ISO's load anticipations could affect the cost performance of deterministic and stochastic DAM SCUC formulations, both individually and in comparison with each other.

A careful study of this robustness issue is beyond the scope of the current study. However, we use our illustrative application to demonstrate how the 8-Zone ISO-NE Test System could be used to implement such a study.

Specifically, we again apply the scenario reduction method [30] to the original 90 two-day hourly load scenarios, except this time we reduce these scenarios to a set $\mathcal{S}^T$ of ten load scenarios of the form $s = (s(z_1), \ldots, s(z_8))$ with associated probabilities. We then simulate "true" loads as realizations from the load-scenario set $\mathcal{S}^T$ rather than from the ISO's anticipated load-scenario set $\mathcal{S}$. Hereafter $\mathcal{S}^T$ is referred to as the *simulated-true load-scenario set*.

The manner in which the ISO's anticipated load-scenario set $\mathcal{S}$ is a biased representation of the simulated-true load-scenario set $\mathcal{S}^T$ is depicted in Fig.1.6, where the two sets are superimposed.

1.4.4 Sensitivity Design

The key treatment factor highlighted in our illustrative application is the system-wide RR level set for the deterministic SCUC formulation. The range of tested RR levels is from 0MW

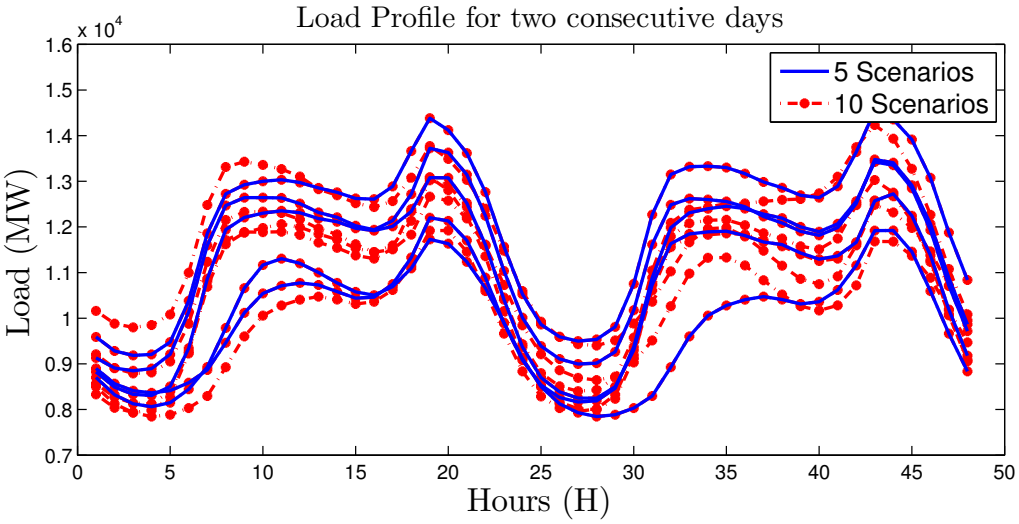

Figure 1.6: Bias in the ISO's load-scenario specifications for the illustrative application, The five scenarios in the ISO's anticipated load-scenario set $\mathcal{S}$ appear as thick solid blue lines, whereas the ten scenarios in the simulated-true load-scenario set $\mathcal{S}^T$ appear as dash-dot red lines.

to 8,500MW, measured in power terms, or from 0% to 61% of peak load for the tested month of March.

The performance metric for our illustrative application is (second-day) expected cost saving, calculated as the (second-day) percentage difference in expected total energy cost when the ISO switches from a deterministic to a stochastic DAM SCUC formulation. As detailed in Section 1.4.2, total energy cost is a summation of start-up, no-load, shut-down, dispatch, and load curtailment costs. The no-load, start-up, and shut-down costs are UC costs that arise from DAM SCUC solutions, whereas the dispatch and load curtailment costs are real-time costs that arise from RTM SCED solutions; see Fig. 1.7.

For each tested RR level, (second-day) expected cost saving is calculated as follows. First, select a load scenario sj from among the ten load scenarios in $\mathcal{S}^T$ to be the simulated-true load for the next two days. Second, calculate the total energy cost that would be realized over each of the the next two days, given RR and sj, assuming the ISO uses the stochastic DAM SCUC formulation conditional on its anticipated load-scenario set $\mathcal{S}$. Third, calculate the total energy cost that would be realized over each of the next two days, given RR and sj, assuming the

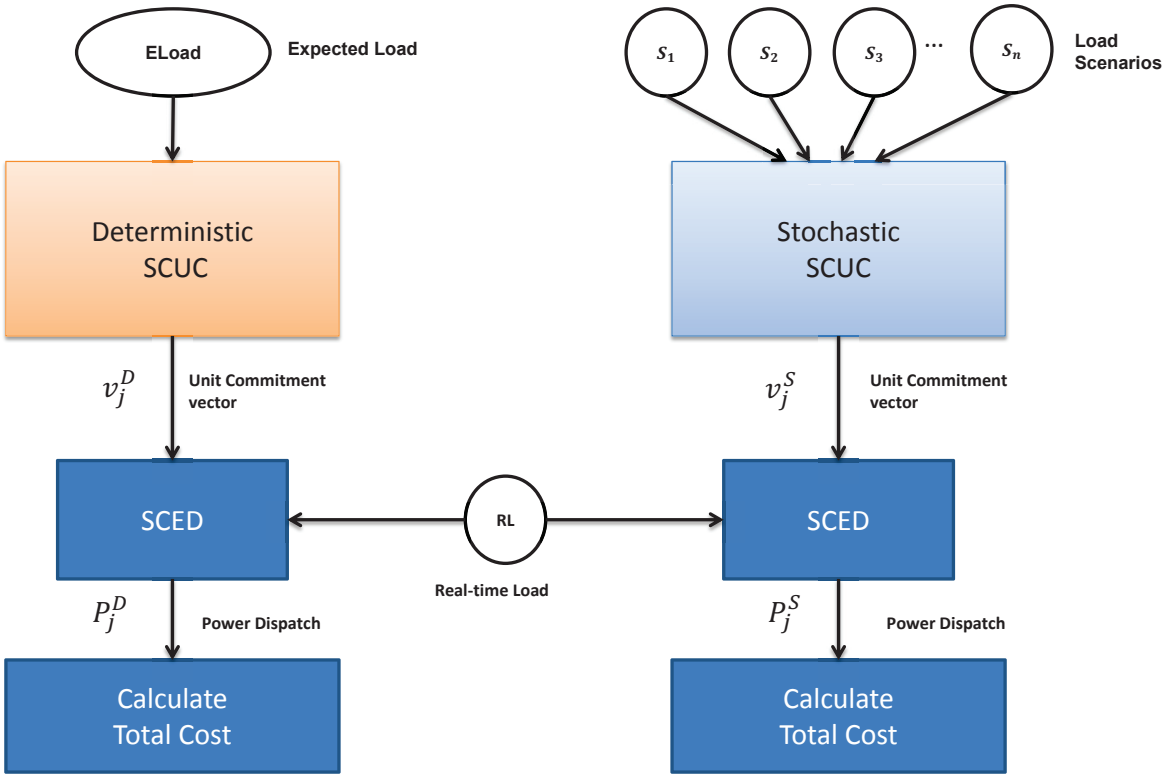

Figure 1.7: Sensitivity testing procedure

ISO uses the deterministic DAM SCUC formulation conditional on the expected load scenario $\bar{s}$ constructed from his anticipated load-scenario set $\mathcal{S}$.

Fourth, letting $\text{TC}_{RR,sj}(\text{Det})$ and $\text{TC}_{sj}(\text{Sto})$ denote the total energy cost resulting on the second day from the implementation of the deterministic and stochastic DAM SCUC formulations, conditional on RR and sj, calculate the (second-day) *Cost Saving* that would result from a switch from a deterministic to a stochastic DAM SCUC, given RR and sj, as follows:

$$\text{CS}_{RR,sj} = \frac{\text{TC}_{RR,sj}(\text{Det}) - \text{TC}_{sj}(\text{Sto})}{\text{TC}_{RR,sj}(\text{Det})} \times 100\% \tag{1.5}$$

Fifth, multiply $\text{CS}_{RR,sj}$ by the probability π^{sj} assigned to the occurrence of sj. Finally, repeat these same steps for each of the ten load scenarios $s1, \ldots, s10$ in $\mathcal{S}^T$, and calculate the (second-day) *expected cost saving*, given RR, as

$$\text{Exp. CS}_{RR} = \sum_{j=1}^{10} \pi^{sj} \text{CS}_{RR,sj} \tag{1.6}$$

1.4.5 Software Implementation

All simulations for our illustrative application were implemented by running the AMES (V4.0) test bed [2] on an Intel(R) Core(TM) 2 Duo CPU E8400 @ 3Ghz machine. AMES (V4.0) uses 64-bit versions of Java (v1.8.0_25), Coopr (v3.4.7842), Python (v2.7.8), MatLab(v2014a) and CPLEX Studio (v12.51). Two threads were used to solve the unit commitment optimization problem.

1.5 Key Findings for the Illustrative Application

This section reports results for the illustrative application described in Section 1.4. A key finding is that the expected cost saving (1.6) resulting from a switch from a deterministic to a stochastic DAM SCUC formulation displays a U-shaped variation as the reserve requirement RR for the deterministic DAM SCUC formulation is successively increased.

Specifically, as shown in the seventh column of Table 1.5 and depicted in Fig. 1.8, Exp. CS_{RR} initially remains relatively flat as the reserve requirement RR is increased from 0% to 18% of peak load. As RR continues to increase, however, Exp. CS_{RR} declines until RR reaches the 25%

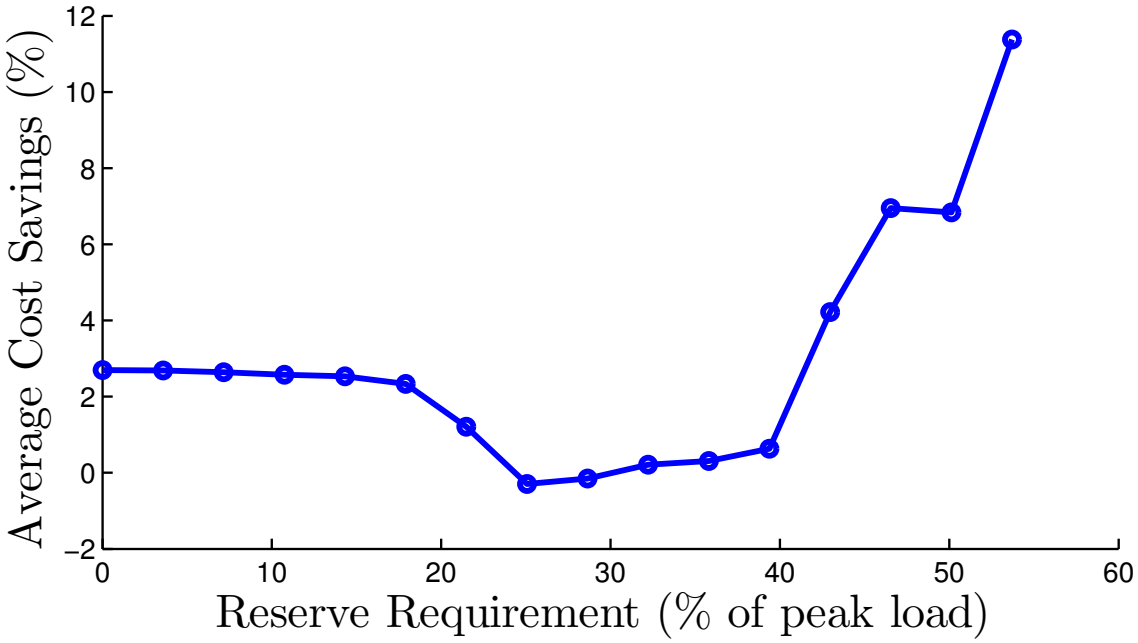

Figure 1.8: Expected cost saving (%) as the reserve requirement (RR) for deterministic DAM SCUC increases from 0% to 54% of peak load for the tested month of March

"sweet spot" for the deterministic DAM SCUC formulation. At this sweet spot, Exp. CS_{RR} turns negative, implying that deterministic SCUC actually outperforms stochastic SCUC in terms of expected total energy costs. However, as RR continues to increase, Exp. CS_{RR} again turns positive and subsequently exhibits a dramatic increase.

In interpreting these results, it is important to consider the standard deviations for expected cost saving reported in the final column of Table 1.5. These standard deviations indicate that the two DAM SCUC formulations do not actually result in *statistically* meaningful differences in expected total energy costs until the RR level for deterministic SCUC exceeds 36%.

Columns three through six in Table 1.5 report the sources of the expected cost saving in column seven, broken out by type of cost (start-up, shut-down, no-load, dispatch). These results reveal that, at low RR levels, a switch from a deterministic to a stochastic DAM SCUC formulation results in a positive expected cost saving with respect to dispatch costs but a negative expected cost saving with respect to start-up, shut-down, and no-load costs. Conversely, at high RR levels a switch from a deterministic to a stochastic DAM SCUC formulation results

Table 1.5: Cost saving by type of cost

RR (MW)	RR (% peak load)	Exp. $CS_{StartUp}$ ($)	Exp. $CS_{ShutDown}$ ($)	Exp. CS_{NoLoad} ($)	Exp. $CS_{Dispatch}$ ($)	Exp. CS_{RR} (%)	Std. CS_{RR} (%)
0	0	-52895.04	-957.90	-52228.42	670739.57	2.70	5.61
500	4	-52895.04	-957.90	-56364.85	672817.21	2.69	5.59
1000	7	-52895.04	-957.90	-56365.13	665961.40	2.64	5.58
1500	11	-52674.25	-960.00	-56367.58	651982.74	2.57	5.42
2000	14	-52895.04	-957.90	-56367.08	646205.25	2.53	5.39
2500	18	-51622.29	-932.43	-55116.10	609888.50	2.33	5.23
3000	21	-33395.04	-594.57	-41302.85	314175.47	1.21	3.72
3500	25	-39110.68	-708.87	-24764.81	84770.44	-0.30	1.16
4000	29	-17683.82	-353.66	1376.09	9797.53	-0.15	0.32
4500	32	-17651.50	-253.02	36212.88	-6072.44	0.21	0.63
5000	36	-12901.50	-158.02	66728.67	-36865.12	0.31	0.63
5500	39	2642.13	32.84	137292.27	-108595.63	0.63	0.55
6000	43	97217.88	1952.85	338930.90	-214583.16	4.22	2.08
6500	47	178901.50	3429.35	556779.82	-367302.19	6.95	2.21
7000	50	178299.17	3035.86	788327.57	-589487.46	6.84	3.50
7500	54	308679.87	1916.91	1088101.44	-743824.36	11.38	4.30
8000	57	411134.36	3921.26	1477314.68	-710729.52	18.37	6.92
8500	61	502400.47	7895.72	2127312.97	-968051.58	24.13	7.74

in a positive expected cost saving with respect to start-up, shut-down, and no-load costs but a negative expected cost saving with respect to dispatch costs.

To understand more fully the disaggregated expected cost saving results reported in Table 1.5, it is necessary to consider more carefully the cost trade-offs under deterministic versus stochastic DAM SCUC formulations as the RR level for deterministic SCUC increases.

Consider, first, the case in which the ISO implements a stochastic DAM SCUC optimization. By construction, the ISO will then commit enough generation in the DAM to ensure load balancing for each real-time load scenario in its anticipated load-scenario set $\mathcal{S}$, no matter how dispersed or improbable these scenarios might be. Consequently, the need to dispatch additional generation (or curtail load) in real time will tend to be reduced, assuming the ISO's anticipated load scenarios are sufficiently accurate depictions of the simulated-true load scenarios in $\mathcal{S}^T$. On the other hand, the ISO will tend to incur high UC costs because he commits sufficient generation in the DAM to balance every one of his anticipated load scenarios.

Next consider the case in which the ISO implements a deterministic DAM SCUC optimization. In this case the ISO does not consider that actual real-time loads might differ from DAM-forecasted loads (i.e., from DAM LSE demand bids). In particular, the ISO does not consider that it might be necessary to dispatch additional generation in real time to balance

higher-than-forecasted loads. Consequently, once the ISO commits enough generation in the DAM to balance DAM-forecasted loads (i.e., to satisfy power balance constraints), the ISO will meet his RR constraints by committing generators in the order of their UC costs, from lowest to highest, regardless of their dispatch costs.

In particular, then, at low RR levels, implementation of the deterministic DAM SCUC results in a lower commitment of generation in comparison with the implementation of the stochastic DAM SCUC. However, implementation of the deterministic DAM SCUC incurs the risk of having to dispatch peaker units with high dispatch costs in real time, a risk that increases with increases in the dispersion of realized loads around their DAM-forecasted values. It thus incurs lower UC costs than stochastic DAM SCUC, but it also incurs higher expected dispatch costs than stochastic DAM SCUC.

Conversely, at high RR levels, implementation of the deterministic DAM SCUC results in a higher commitment of generation in comparison with the implementation of the stochastic DAM SCUC. In this case both the deterministic DAM SCUC and the stochastic DAM SCUC avoid the need to dispatch any additional generation in real time (including any peaker units); but the deterministic DAM SCUC incurs higher expected UC costs due to its higher overall total committed capacity.

As the above observations suggest, the expected cost saving results reported in Table 1.5 depend strongly on the dispersion of the possible next-day loads as well as on the available mix of the generation fleet. A closer examination of specific simulation runs helps to clarify the nature of this dependence.

We first select a particular simulated-true load scenario $s^* \in \mathcal{S}^T$ for which realized (i.e., simulated-true) load is higher than the corresponding DAM-forecasted load in each hour. Three simulation runs are conducted for s^* under three different RR specifications: namely, RR=0%, RR=29%, and RR=47%. Second-day outcomes are plotted in Figs. 1.9, 1.10, and 1.11 for each of these three simulation runs.[12]

[12]In Figs. 1.9 through 1.13, the solid (red) line denotes total committed capacity under stochastic DAM SCUC, and the dashed (blue) line denotes total committed capacity under deterministic DAM SCUC. The line consisting of alternating dots and dashes denotes DAM-forecasted loads. The bars denote dispatch levels. For each hour, the left-side bar denotes the dispatch level under deterministic DAM SCUC, and the right-side bar denotes the dispatch level under stochastic DAM SCUC; these bars have equal heights because each dispatch equals realized

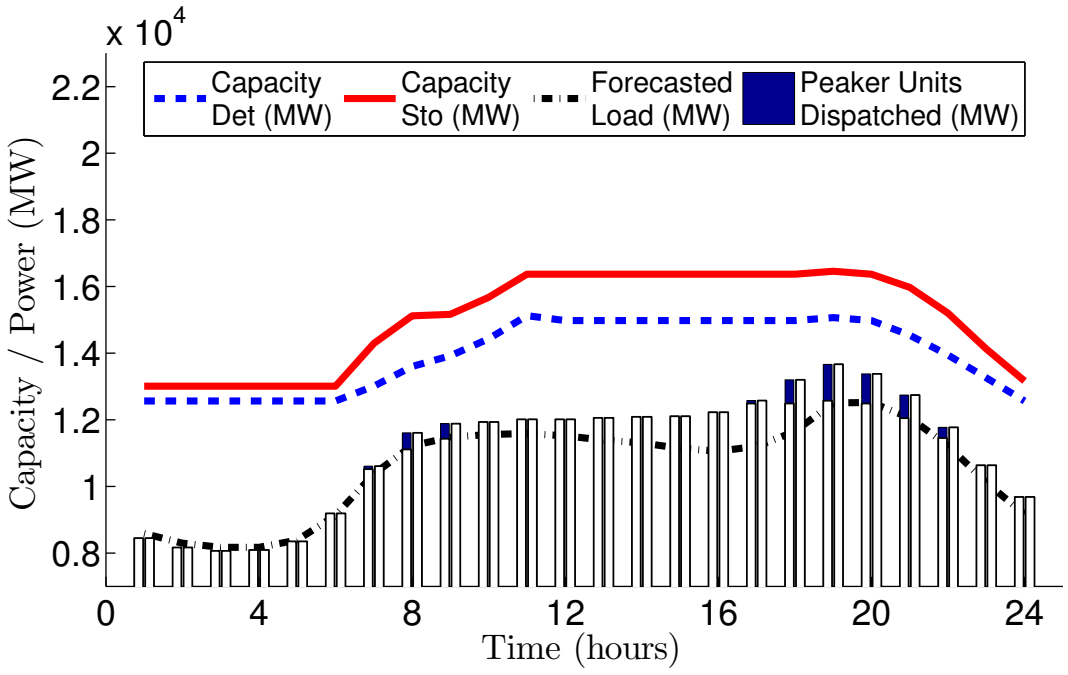

Figure 1.9: Outcomes for the second day, given RR = 0% and s^* with realized load greater than forecasted load in each hour: Cost Saving = 7.33%

In Fig. 1.9, with RR=0%, the total committed capacity is higher under stochastic DAM SCUC since this formulation accounts for variance in loads whereas the deterministic DAM SCUC commits only enough generation to balance DAM-forecasted loads. In particular, for the deterministic DAM SCUC, the ISO bets, incorrectly, that realized (i.e., simulated true) loads will not exceed DAM-forecasted loads. The ISO is then forced to call on peaker units with very-high dispatch costs to meet higher-than-forecasted real-time loads. A switch to a stochastic DAM SCUC would result in a 7.33% cost saving for this case.

In Fig. 1.10, with RR increased to 29%, the total committed capacity is slightly higher under the deterministic DAM SCUC. The ISO implementing the deterministic DAM SCUC is now forced to commit more generation capacity because of the higher RR level, in comparison to the previous case with RR = 0%. However, this amount of committed generation is similar to the amount of committed generation that would be committed under a stochastic DAM SCUC. Subsequently, when realized loads turn out to be higher than DAM-forecasted loads, the ISO

load for that hour. Finally, blackened areas (if any) at the top of a left-side bar or right-side bar indicates a dispatch of peaker generation units under deterministic or stochastic DAM SCUC, respectively.

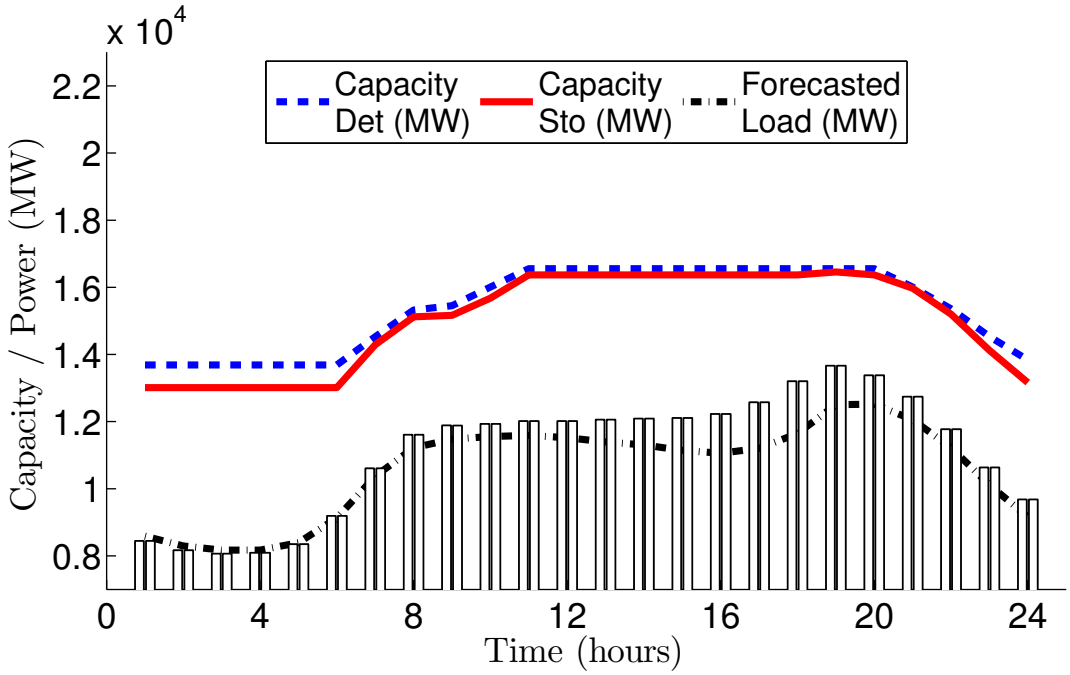

Figure 1.10: Outcomes for the second day, given RR = 29% and s^* with realized load greater than forecasted load in each hour: Cost Saving = -0.07%

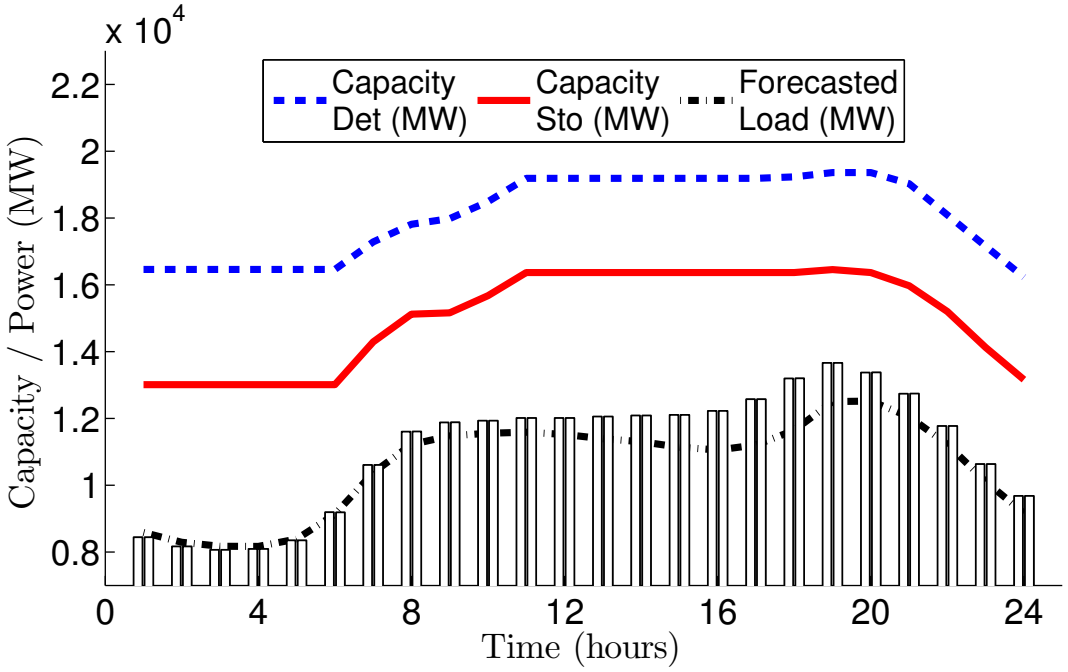

Figure 1.11: Outcomes for the second day, given RR = 47% and s^* with realized load greater than forecasted load in each hour: Cost Saving = 10.03%

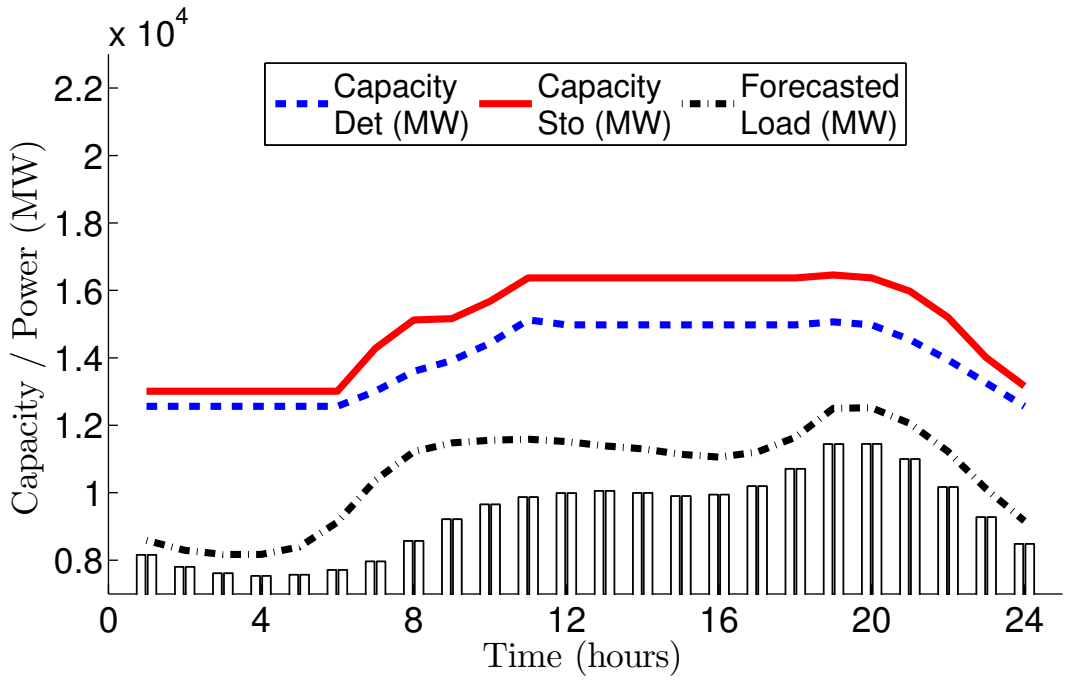

Figure 1.12: Outcomes for the second day, given RR = 0% and s^{**} with realized load less than forecasted load in each hour: Cost Saving = -1.49%

calls on its committed generation to balance realized loads. A switch to a stochastic DAM SCUC would result in a negative cost saving of -0.07% for this case.

In Fig. 1.11, with RR increased all the way up to 47%, the ISO implementing a deterministic DAM SCUC has plenty of unencumbered capacity from committed generation to call on as reserve when realized loads exceed forecasted loads. However, the ISO also pays an excessive amount of UC costs for this generation. A switch to a stochastic DAM SCUC would result in a 10.03% cost saving in this case.

Now consider the selection of a particular simulated-true load scenario $s^{**} \in \mathcal{S}^T$ for which realized (i.e., simulated-true) load is *lower* than the corresponding DAM-forecasted load in each hour. Outcomes for two simulation runs conducted for s^{**} under two different RR levels, RR=0% and RR=47%, are depicted in Figs. 1.12 and 1.13, respectively.

Under either RR level, both deterministic and stochastic DAM SCUC commit enough generation capacity to meet realized loads. Under RR=0%, the stochastic DAM SCUC commits more generation capacity; hence, the stochastic DAM SCUC has higher UC costs than the de-

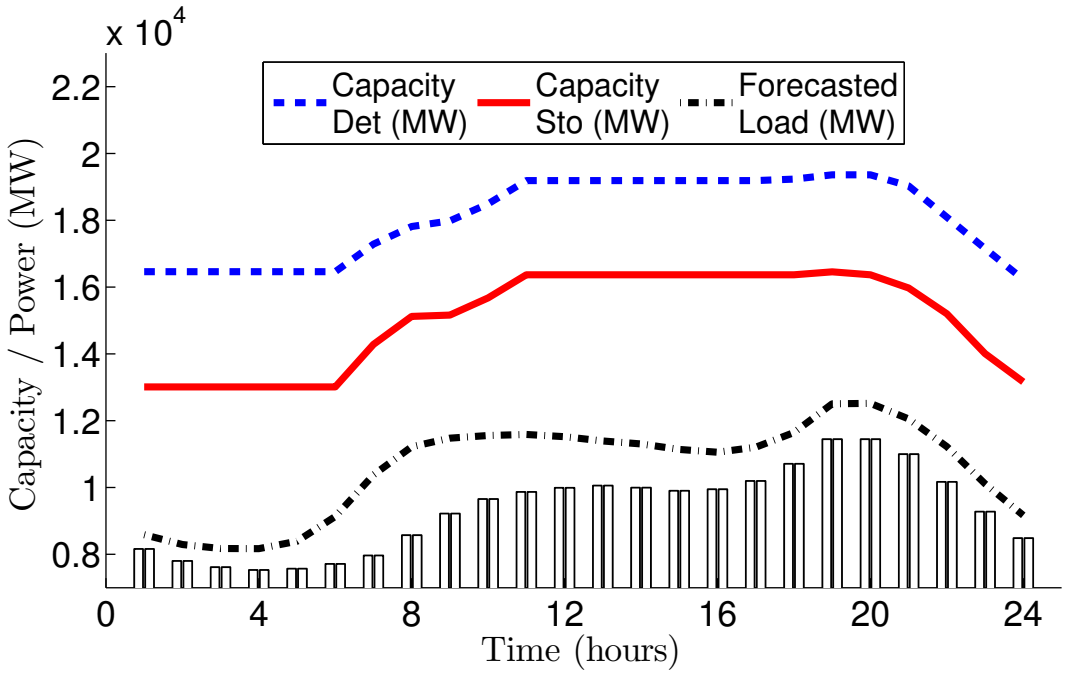

Figure 1.13: Outcomes for the second day, given RR = 47% and s^{**} with realized load less than forecasted load in each hour: Cost Saving = 4.73%

terministic DAM SCUC, and a switch from a deterministic to a stochastic DAM SCUC would result in a negative cost saving of -1.49% for this case. On the other hand, under RR=47%, it is the deterministic DAM SCUC that commits more generation and pays more UC costs; hence, a switch from a deterministic to a stochastic DAM SCUC would result in a positive cost saving of 4.73% for this case.

1.6 Concluding Remarks for Chapter 1

To our knowledge, the 8-Zone ISO-NE Test System is the first open-source release of an empirically-grounded test system that permits the systematic study of power market design and performance issues for ISO-NE by means of systematic fast-execution computational experimentation.

For example, in Section 1.5 this test system is used to conduct comparative performance studies of alternative DAM SCUC optimization formulations for the improved handling of uncertainties when the ISO's anticipated load scenarios are biased representations of possible

future load realizations. The reported findings reveal that the expected cost saving arising from a switch from a deterministic to a stochastic DAM SCUC formulation exhibits a U-shaped dependence on the reserve requirement (RR) for deterministic SCUC. The exact form of this U-shape depends in a rather complicated way on the available generation mix and on the dispersion of the possible next-day loads. Indeed, for RR levels in a neighborhood of the U-turn point, cost saving can be negative, meaning the deterministic DAM SCUC formulation outperforms the stochastic DAM SCUC formulation.

These findings demonstrate that simulation studies with small-scale test systems, such as the 8-Zone ISO-NE Test System, can help to clarify the precise conditions under which various DAM SCUC formulations are cost effective. In ongoing work we are extending this application to test the robustness of our findings to alternative specifications of the generation mix, including the addition of non-dispatchable wind power (treated as negative load) with its concomitant effects on the dispersion of net loads.

The 8-Zone ISO-NE Test System can also be used to test the effectiveness of alternative forms of reserve requirements (e.g., local versus system wide), price cap constraints, and a variety of other market design features. Another critical issue that could be explored is the extent to which market operating procedures are susceptible to manipulation for market power gain through strategic bids and offers. As noted in Section 1.2, the test system is implemented via AMES (V4.0) [2], which permits GenCos and LSEs to be modeled as learning agents able to change their offer/bid methods over time on the basis of past experiences.

Through such exploratory studies, the 8-Zone ISO-NE Test System can facilitate understanding of current market operations. It can also function as a computational laboratory for the development of new ideas for improving these operations, and provide cautionary indications of possible adverse consequences that might result from these intended improvements.

The empirical grounding of the 8-Zone ISO-NE Test System in the structure and empirical conditions for the ISO-NE energy region could be viewed as a limitation in that it appears to narrow its range of application. Researchers wishing to apply the test system to an energy region other than ISO-NE would need to introduce a number of changes in the structural specifications and/or benchmark configurations for the test system to match the rules of operation

and empirical conditions of this alternative energy region. Moreover, the test system currently models a single ISO-managed energy region, without consideration of flows with neighboring energy regions. In reality, an ISO must carefully consider power flows between its own region and neighboring energy regions.

However, as stressed throughout this study, the 8-Zone ISO-NE Test System is implemented via the modular and extensible AMES (V4.0) test bed. This should greatly ease the burden of restructuring the test system to permit the study of alternative energy regions, or to permit the study of seaming issues, if a user desires to do so.

A key limitation of the test system is its relatively small scale, which limits it to exploratory studies. The test system does not provide a test environment with suitably-high fidelity for testing the efficacy of proposed system modifications intended for immediate commercial application.

Appendix : Nomenclature and Mathematical Formulation

Nomenclature

a_g	Production cost coefficient for generator g
b_g	Production cost coefficient for generator g
$B(\ell)$	Inverse of reactance (pu) on line ℓ
$C_{D,g}(k)$	Shut-down cost of g in hour k
$C_{N,g}(k)$	No-load cost of g in hour k
$C_{U,g}(k)$	Start-up cost of g in hour k
$C^s_{P,g}(k)$	Dispatch cost of g in hour k, given s
$c_{D,g}$	Shut-down cost coefficient for g
$c_{N,g}$	No-load cost coefficient for g
$c_{S,g}$	Cold-start cost coefficient for g
$E(\ell)$	End zone for line ℓ
f_ℓ^{max}	Power limit for transmission line ℓ
$\mathcal{G}$	Set of all generators g

$\mathcal{G}(z)$	Set of generators g located in zone z
$H_g(k)$	Hot-start indicator for g: 1 if hot start in hour k; 0 otherwise
$h_{S,g}$	Hot-start cost coefficient for g required to satisfy $h_{S,g} \leq c_{S,g}$
K	Set of indices k for hours of operation
$L^s(z,k)$	Zone-z load in hour k, given s
$\mathcal{L} \subset \mathcal{Z} \times \mathcal{Z}$	Set of transmission lines ℓ
$\mathcal{L}_O(z)$	Subset of lines $\ell \in \mathcal{L}$ originating at zone z
$\mathcal{L}_E(z)$	Subset of lines $\ell \in \mathcal{L}$ ending at zone z
$O(\ell)$	Originating zone for line ℓ
$p_g^s(k)$	Power output of g for hour k, given s
$\overline{p}_g^s(k)$	Maximum available power output for g in hour k, given s
$\overline{P}_g$	Maximum power output for g
$\underline{P}_g$	Minimum power output for g
$R_{D,g}$	Ramp-down limit (MW/Δk) for g
$RT_{D,g}$	$\min\{\overline{P}_g, R_{D,g}\Delta k\}$ (MW)
$R_{U,g}$	Ramp-up limit (MW/Δk) for g
$RT_{U,g}$	$\min\{\overline{P}_g, R_{U,g}\Delta k\}$ (MW)
$R_{SD,g}$	Shut-down ramp limit (MW/Δk) for g
$RT_{SD,g}$	$\min\{\overline{P}_g, R_{SD,g}\Delta k\}$ (MW)
$R_{SU,g}$	Start-up ramp limit (MW/Δk) for g
$RT_{SU,g}$	$\min\{\overline{P}_g, R_{SU,g}\Delta k\}$ (MW)
$RR(k)$	System-wide reserve requirement in hour k for deterministic DAM SCUC
S	Set of scenarios s
S_o	Positive base power (in three-phase MVA)
$T_{C,g}$	No. of cold-start hours for g
$T_{\text{off},g}$	No. of hours that g must be initially offline if $0 > \hat{v}_g(0)$; 0 if $0 < \hat{v}_g(0)$
$T_{\text{on},g}$	No. of hours that g must be initially online if $0 < \hat{v}_g(0)$; 0 if $0 > \hat{v}_g(0)$
$T_{D,g}$	Minimum down-time for g
$T_{U,g}$	Minimum up-time for g

$v_g(k)$	g's on/off status in hour k
$\hat{v}_g(0)$	g's down-time/up-time status at time 0 [13]
$w_\ell^s(k)$	Power on line ℓ in hour k, given s
$\mathcal{Z}$	Set of zones z
$\alpha^s(z,k)$	Power-balance slack term at zone z in hour k, given s
Δk	Time-period length (one hour)
$\gamma^s(z,k)$	Absolute value of $\alpha^s(z,k)$
Λ	Penalty weight for non-zero slack terms
π^s	Probability of scenario s
$\theta_z^s(k)$	Voltage angle (radians) at zone z in hour k, given s

Stochastic Unit Commitment Formulation

Objective function:

$$\sum_{k\in K}\sum_{g\in\mathcal{G}}[C_{U,g}(k)+C_{N,g}(k)+C_{D,g}(k)] + \sum_{s\in S}\pi^s\sum_{k\in K}\sum_{g\in\mathcal{G}}C_{P,g}^s(k)+\Lambda\sum_{s\in S}\pi^s\sum_{z\in\mathcal{Z}}\sum_{k\in K}\gamma^s(z,k) \tag{1.7}$$

ISO decision variables:

$$v_g(k),\ p_g^s(k),\ \theta_z^s(k),\quad \forall z\in\mathcal{Z}, g\in\mathcal{G}, k\in K, s\in S \tag{1.8}$$

ISO decision variable bound constraints:

$$v_g(k)\in\{0,1\} \qquad \forall g\in\mathcal{G}, k\in K \tag{1.9}$$

$$0\le p_g^s(k)\le \overline{P}_g \qquad \forall g\in\mathcal{G}, k\in K, s\in S \tag{1.10}$$

$$-\pi\le\theta_z^s(k)\le\pi \qquad \forall z\in\mathcal{Z}, k\in K, s\in S \tag{1.11}$$

[13] A positive (negative) value for $\hat{v}_g(0)$ indicates the number of hours prior to and including hour 0 that generator g has been turned on (off). Note that $\hat{v}_g(0)$ cannot be zero-valued.

Scenario-conditioned power balance constraints for each zone:

$$\sum_{g\in\mathcal{G}(z)} p_g^s(k) + \sum_{\ell\in\mathcal{L}_E(z)} w_\ell^s(k) + \alpha^s(z,k) \tag{1.12}$$
$$= L^s(z,k) + \sum_{\ell\in\mathcal{L}_O(z)} w_\ell^s(k)\ ;$$

$$\alpha^s(z,k) = \alpha^{+,s}(z,k) - \alpha^{-,s}(z,k)\,; \tag{1.13}$$

$$\gamma^s(z,k) = \alpha^{+,s}(z,k) + \alpha^{-,s}(z,k) \tag{1.14}$$

$$\forall z\in\mathcal{Z}, k\in K, s\in S \tag{1.15}$$

Scenario-conditioned capacity constraints for each $g\in\mathcal{G}$:

$$\underline{P}_g v_g(k) \le p_g^s(k) \le \bar{p}_g^s(k), \qquad \forall k\in K, s\in S \tag{1.16}$$

$$0 \le \bar{p}_g^s(k) \le \bar{P}_g v_g(k), \qquad \forall k\in K, s\in S \tag{1.17}$$

Scenario-conditioned limit constraints for each line $\ell\in\mathcal{L}$:

$$w_\ell^s(k) = S_o B(\ell)\left[\theta^s_{O(\ell)}(k) - \theta^s_{E(\ell)}(k)\right], \tag{1.18}$$

$$-f_\ell^{max} \le w_\ell^s(k) \le f_\ell^{max}, \qquad \forall k\in K, s\in S \tag{1.19}$$

Scenario-conditioned ramp constraints for each $g\in\mathcal{G}$:

$$\bar{p}_g^s(k) \le p_g^s(k-1) + RT_{U,g}[v_g(k-1)]$$
$$+ RT_{SU,g}[v_g(k) - v_g(k-1)] + \bar{P}_g[1 - v_g(k)],$$
$$\forall k\in K, s\in S \tag{1.20}$$

$$\bar{p}_g^s(k) \le \bar{P}_g v_g(k+1) + RT_{SD,g}[v_g(k) - v_g(k+1)],$$
$$\forall k = 1,\cdots,(|K|-1), \forall s\in S \tag{1.21}$$

$$p_g^s(k-1) - p_g^s(k) \le RT_{D,g} v_g(k)$$
$$+ RT_{SD,g}[v_g(k-1) - v_g(k)]$$
$$+ \bar{P}_g[1 - v_g(k-1)],$$
$$\forall k\in K, s\in S \tag{1.22}$$

Hot start-up constraints for each $g \in \mathcal{G}$:

$$H_g(k) = 1, \qquad 1 \le k \le T_{C,g} : (k - T_{C,g}) \le \hat{v}_g(0) \tag{1.23}$$

$$H_g(k) \le \sum_{t=1}^{k-1} v_g(t), \; 1 \le k \le T_{C,g} : (k - T_{C,g}) > \hat{v}_g(0) \tag{1.24}$$

$$H_g(k) \le \sum_{t=k-T_{C,g}}^{k-1} v_g(t), \quad \forall k = (T_{C,g} + 1), \ldots, |K| \tag{1.25}$$

Start-up cost constraints for each $g \in \mathcal{G}$:

$$\begin{aligned} C_{U,g}(k) &= \max\{0, U_g(k)\}\,; \\ U_g(k) &= c_{S,g} - [c_{S,g} - h_{S,g}] H_g(k) \\ &\quad - c_{S,g}\big[1 - [v_g(k) - v_g(k-1)]\big], \qquad \forall k \in K \end{aligned} \tag{1.26}$$

No-load cost constraints for each $g \in \mathcal{G}$:

$$C_{N,g}(k) = c_{N,g} v_g(k), \; \forall k \in K \tag{1.27}$$

Shut-down cost constraints for each $g \in \mathcal{G}$:

$$\begin{aligned} C_{D,g}(k) &= \max\{0, D_g(k)\}\,; \\ D_g(k) &= c_{D,g}[v_g(k-1) - v_g(k)], \qquad \forall k \in K \end{aligned} \tag{1.28}$$

Minimum up-time constraints for each $g \in \mathcal{G}$:

$$\sum_{k=1}^{T_{\text{on},g}} [1 - v_g(k)] = 0 \text{ if } T_{\text{on},g} \ge 1\,; \tag{1.29}$$

$$\sum_{n=k}^{k+T_{U,g}-1} v_g(n) \ge T_{U,g}[v_g(k) - v_g(k-1)],$$

$$\forall k = (T_{\text{on},g} + 1), \cdots, (|K| - T_{U,g} + 1)\,; \tag{1.30}$$

$$\sum_{n=k}^{|K|} (v_g(n) - [v_g(k) - v_g(k-1)]) \ge 0,$$

$$\forall k = (|K| - T_{U,g} + 2), \cdots, |K| \tag{1.31}$$

Minimum down-time constraints for each $g \in \mathcal{G}$:

$$\sum_{k=1}^{T_{\text{off},g}} v_g(k) = 0 \text{ if } T_{\text{off},g} \geq 1\,; \tag{1.32}$$

$$\sum_{n=k}^{k+T_{D,g}-1} [1 - v_g(n)] \geq T_{D,g}[v_g(k-1) - v_g(k)],$$

$$\forall k = (T_{\text{off},g} + 1), \cdots, (|K| - T_{D,g} + 1)\,; \tag{1.33}$$

$$\sum_{n=k}^{|K|} \left[1 - v_g(n) - [v_g(k-1) - v_g(k)]\right] \geq 0,$$

$$\forall k = (|K| - T_{D,g} + 2), \cdots, |K| \tag{1.34}$$

Voltage angle constraints for angle reference zone 1:

$$\theta_1^s(k) = 0, \quad \forall k \in K, s \in S \tag{1.35}$$

CHAPTER 2: IMPROVING PERFORMANCE OF UNIT COMMITMENT AND ECONOMIC DISPATCH FORMULATIONS

Dheepak Krishnamurthy

Abstract

As part of the day-ahead market clearing process, ISOs solve a challenging Security Constrained Unit Commitment (SCUC) problem. With a growing footprint and active participation from market players, solving day-ahead market unit commitment in a performant and accurate manner is becoming more crucial. Additionally, capturing the complexity of these real world processes in simulation tools is extremely valuable to explore new algorithms for increasing performance. This chapter discusses the implementation of improvements to the Security Constrained Unit Commitment (SCUC) formulation and the Security Constrained Economic Dispatch (SCED) for a more accurate and efficient simulation of power market operations in Agent-based Modeling of Electricity Systems (AMES). Firstly, this chapter shares an iterative algorithm integrating the DC Optimal Power Flow (OPF) based SCUC solver and an AC Power Flow (ACPF) solver as a means to improve the reliability of a solution for large power systems. Next, this chapter discusses an alternate implementation for both SCUC and SCED formulations that uses Power Transfer Distribution Factors (PTDF) and characterises the performance of this alternate formulation. This alternate implementation has also been bundled into a research capable toolbox called Power System Simulation Toolbox (PSST) and the toolbox along with other improvements have been released as a new version of AMES (AMES (V4.0) [31]). Finally, two additional improvements to the SCUC formulation in AMES (V4.0) are explored in a sensitivity analysis by measuring the effect on the objective function of a standard SCUC formulation. This analysis was performed to verify - 1) the effect of changing rolling horizon time period for SCUC formulations and, 2) the effect of improved fidelity in piecewise linear

approximations of cost curves. Lastly, a verification of the SCUC and SCED formulations in AMES (V4.0) is detailed.

2.1 Introduction

Modeling tools demand more efficient and accurate tools to support decision making for resource scheduling in large complex power systems. Market operation problems are solved in power systems to determine when to startup or shutdown generating units, and to decide how to dispatch these generating units to meet system demand and spinning reserve requirements. These decisions are optimized minimizing overall operations cost or maximizing social welfare while under generation constraints like production limits, ramping limits, minimum up times, minimum down times, and system constraints like line limits, voltage limits and angle limits. Generation scheduling problems are solved by Independent System Operators (ISO) in electricity markets, using market participants bids and offers to maximize social welfare. System operators ensure system reliability by utilizing Security Constrained optimization models, namely a unit commitment and economic dispatch model that is extended to include transmission network constraints. Simulating real world operations more accurately or efficiently can result in better decision making tools.

This chapter explores various improvements that can be made to a standard SCUC and SCED formulation in order to improve performance in terms of solve time and accuracy. Section 2.2 describes the updates made to AMES (V4.0) in order to test these various improvements. This section also describes the two current implementations of SCUC and SCED solvers in AMES (V4.0) to demonstrate why these changes were necessary. Section 2.3 describes an iterative algorithm that integrates a DC-OPF SCUC solver with an ACPF solver. Next, section 2.4 discusses an alternative implementation of the SCUC and SCED formulation (PTDF formulation), performs a sensitivity analysis on two parameters, and compares the results to the current formulation ($B \times \theta$ formulation). Finally, sections 2.5 and 2.6 discuss the effect of the implementation of a rolling horizon time period and the effect of number of bid segments in the cost curve for generators on the objective function of a standard SCUC formulation.

2.2 Description of updates to AMES

Significant changes were made to better represent a model of the wholesale power market. These changes will be released as a version update, in the form of AMES (V4.0)[1] [31]. The following is a summary of the description of the changes from AMES (V2.06). The full comprehensive list of changes in AMES (V4.0) is described as part of the documentation [31].

1. AMES (V2.06) employs a DCOPFJ algorithm to solve for optimal dispatches in a Day-Ahead Market (DAM). AMES (V4.0) incorporates a new DAM interface. This DAM interface allows switching between different solvers. The current solvers supported are:
   (a) Deterministic and Stochastic SCUC using Pyomo
   (b) Deterministic SCUC using PSST and Pyomo
2. AMES (V4.0) also incorporates hourly Real-Time Market (RTM) interface. This RTM interface allows switching between different solvers. The current solvers supported are:
   (a) Deterministic SCED using Pyomo
   (b) Deterministic SCED using PSST and Pyomo
3. AMES (V4.0) allows the user to define the following parameters
   (a) Rolling Horizon Period
   (b) Number of pieces in for a Piecewise Linear Cost Curve

Other changes include an improved test case file format reader that includes support for reading of load scenarios, and improved visualization of input and output data.

The DAM interface includes an operation that solves a Security Constrained Unit Commitment (SCUC) formulation of the power system. The detailed formulation is listed in [1] and in the chapter above. The SCUC formulation described in the previous chapter is implemented in Pyomo [32]. Pyomo is a Python-based, open-source optimization modeling language with a diverse set of optimization capabilities. This formulation can be solved as a stochastic or

[1] For the purposes of development and testing of the new features in AMES (V4.0), the learning features of GenCos were turned off.

deterministic formulation using the direct Pyomo solver. The PSST solver interface currently supports deterministic formulations; stochastic formulations are planned to be supported in the future.

2.2.1 Power System Simulation Toolbox (PSST)

Power System Simulation Toolbox (PSST) in Python is a collection of functions developed for rapid, fast-iterative design of models for power systems. It provides a wrapper over Pyomo for SCUC/SCED formulations. PSST allows tailoring the number and type of constraints to build a single model dynamically. It can model interface flow limits, curtailable generation, zonal reserves, storage modeling. It also has the ability to build multiple formulations.

It has allowed for improved maintainability in AMES (V4.0). It also provides integration with existing power flow tools such as PYPOWER/MATPOWER. PSST can be found in the AMES (V4.0) repository [31].

2.2.2 Implementation of Pyomo solver in AMES (V4.0)

Pyomo is an open source software package which supports the definition and solution of optimization applications using the Python scripting language. Pyomo includes Python classes for defining sparse sets, parameters, and variables, which can be used to formulate algebraic expressions that define objectives and constraints. Pyomo can be used to represent linear, mixed-integer, nonlinear, and nonlinear mixed-integer models for large-scale, real-world problems that involve thousands of constraints and variables. This capability is commonly associated with algebraic modeling languages (AMLs) such as AMPL and GAMS. Pyomo models can be analyzed with a wide array of optimization solvers including GLPK, CBC, SCIP, CPLEX, GUROBI, and IPOPT.

Pyomo allows an external program to use system call that can read a Python file (conventionally referred to as "ReferenceModel.py"). This file typically contains sets, parameters, and variables, objective functions and constraints, and describes a formulation of a problem. The model described in this file is typically an "Abstract Model". An "Abstract Model" is a Pyomo construct that describes a model that does not have data in it. When this file is executed, the

"Abstract Model" is constructed that declared the sets, parameters, variables, objective functions and constraints. However, since an "Abstract Model" does not contain data to define the values of sets and parameters, a reference to a separate data file must be included in the system call that contains values for the sets and parameters.

The implementation of the Pyomo solver in AMES (V4.0) is shown in Figure 2.1. For every DAM SCUC solve, AMES (V4.0) writes out a file "AMES.dat" in the current working directory. AMES (V4.0) then issues a system call to run the command `pyomo solve ReferenceModel.py AMES.dat`. As described above, the system call from AMES (V4.0) to solve a model constructed by the "ReferenceModel" requires an argument that links to the file "AMES.dat" that contains data defining the values of the parameters, sets etc. This system call runs Pyomo which in turn builds the abstract model in "ReferenceModel.py" and attaches the data in "AMES.dat" to the "Abstract Model". Once a model has been built, it can be solved using a solver in the environment. When a successful solution has been attained Pyomo returns results to a file, which in turn are read by AMES (V4.0). These results include LMP at all nodes, and unit commitment status and dispatch levels for all generators.

While this implementation is straightforward and easy to understand, it offers little flexibility in solving different formulations, increasing solver accuracy or decreasing solver times. This is addressed by using the PSST solver, as described in the following subsection.

2.2.3 Implementation of PSST solver in AMES (V4.0)

PSST allows additional flexibility over the approach described in section 2.2.2. In the previous approach, AMES (V4.0) uses a system call to Pyomo to solve the model described by the "ReferenceModel.py". Pyomo in turn reads and executes the file "ReferenceModel.py" sequentially, in order to build the model. This rigidity in execution of Pyomo and Python would result in complexity for the development of AMES (V4.0). For example, for AMES (V4.0) to support N number of formulations, there would have to be N independent models that could be solved using Pyomo. This also would not allow for selectively adding constraints.

PSST solves this problem by acting as a wrapper on top of Pyomo for power system optimization problems. PSST reads the data in "AMES.dat" and builds the model in memory.

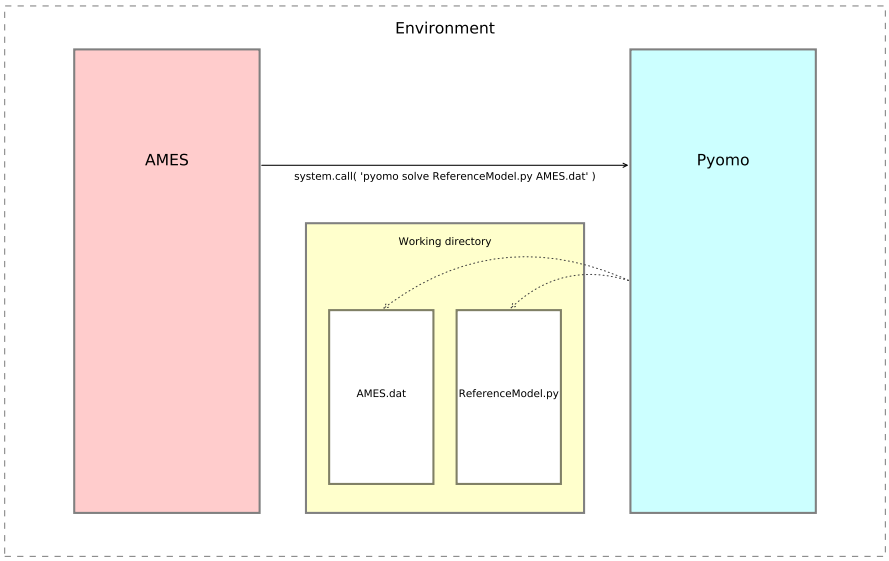

Figure 2.1: Current implementation of AMES (V4.0) Pyomo solver call

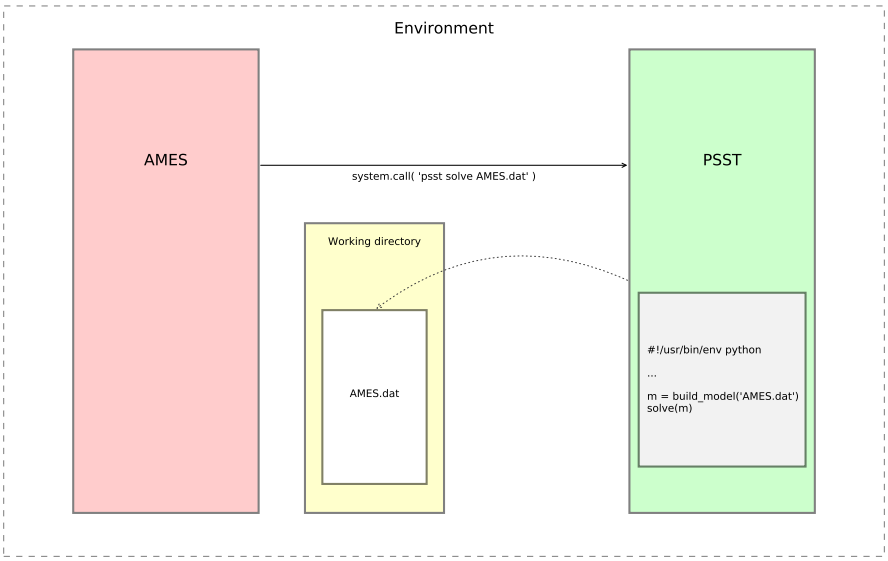

Figure 2.2: Current implementation of AMES (V4.0) PSST solver call

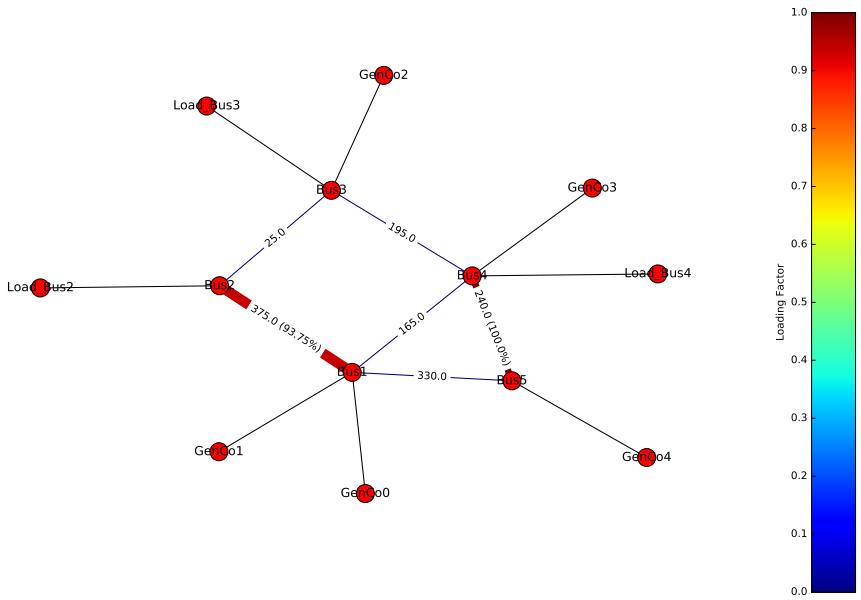

Figure 2.3: Line power in hour 1 for PJM 5 Bus Test System

Since the model is built entirely in memory, the SCUC or SCED formulation solved can be dynamically updated. Another advantage of this approach is that changes, improvements or bug fixes applied to one formulation directly benefit all formulations. This flexible approach also allows for switching on and off different constraints dynamically, without changing the test case data set. This toolbox has allowed exploring methods to iterative solutions that will be beneficial to attain more reliable solutions for large complex SCUC problems. This toolbox has also facilitated a comparison between a PTDF formulation and a $B \times \theta$ formulation. These two capabilities are demonstrated in the following sections.

In addition to the above benefits, PSST has been instrumental in aiding the debugging and development of AMES (V4.0), with the goal of making research faster, more effective and more accessible. Fast prototyping in Python and ability to visualize instantaneous results as seen in Figure 2.3 make it an effective research tool.

2.3 Iterative SCUC with ACPF integration

Typically, system operators are required to serve load in the most cost effective way while maintaining the integrity of the system and maintaining reliability requirements. For a large complex power system, it may be very difficult to achieve a zero MIP gap for DAM SCUC in the preferred amount of time. In order to solve for the unit commitment status and economic dispatch values in large complex systems in a timely manner, an ISO may decide to solve a simplified system. For example, one such simplification may be to remove line constraints thereby aggregating multiple nodes. However, this simplified system may not yield the globally optimal solution. Moreover, these approximations may result in solutions that are infeasible when deployed on a real system. Typically, these always result in a mismatch between solutions from a DC-OPF SCUC and an actual ACPF.

One solution to this problem is to employ an iterative approach. Although this iterative approach may require solving SCUC more than one time, this can lead to additional reliability. ACPF solutions, that have been set up correctly can be used to inform and update the DC-OPF SCUC model and which can then be re-solved for unit commitment and generator dispatch levels. More specifically, a simplified DC-OPF SCUC can be constructed by removing line constraints, and this model can be solved. The power dispatch values from the DC-OPF SCUC can be used as an input to an ACPF algorithm. Then line power flows calculated from ACPF can be used to determine which line constraints would be violated if this DC-OPF SCUC solution were to be deployed. These line constraints are then added back to the DC-OPF SCUC model and the problem is resolved. This iterative approach can provide additional reliability for a large complex power system problem where the full DC-OPF SCUC cannot be solved in the preferred amount of time. The algorithm is described below, as depicted in Figure 2.4. The development of the adaptive dynamic constraint generation feature in PSST has allowed for testing this iterative algorithm.

For the initial step, the line power flow constraints are removed. With no line constraints enabled (i.e. bus angle and line power limit constraints), this effectively reduces the problem to a single node system. This system is then solved with the a DC-OPF SCUC formulation.

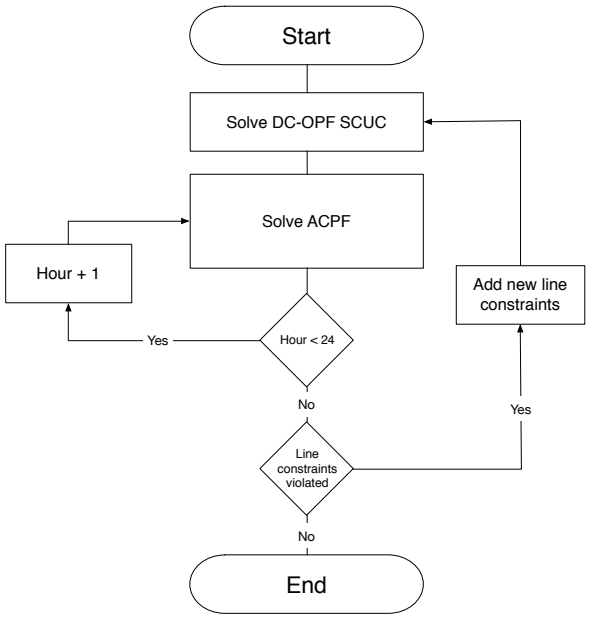

Figure 2.4: Flowchart iterative DC-OPF SCUC and ACPF

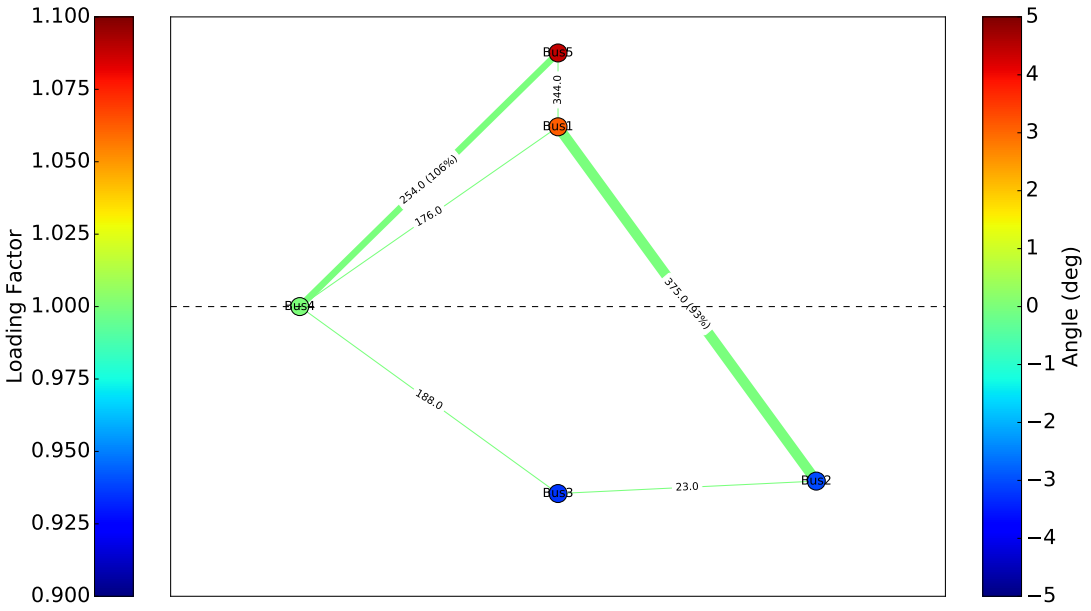

Figure 2.5: Bus angles in hour 1 for PJM 5 Bus Test System for solution without adding line constraints

After the solution is obtained, the forecasted load consumption, generator dispatch levels and unit commitment status from the DC-OPF SCUC solution for every hour are used as an input to solve an ACPF problem. The line power flows from the ACPF solution at each hour are compared to the original line power flow constraints. Figure 2.5 shows line power flows on each branch and voltage angles on each bus if the solution from the SCUC DC-OPF without adding line constraints were deployed to the system. Since no bus angle or line power limit constraints were enabled to calculate this solution, this can result in line violations when deployed in a real world system. An ACPF solution is used to represent the real world system behavior in this study. It can be seen that line flow between Bus 5 and Bus 4 exceeds the rated capacity of the line, and hence it is observed that this solution is not feasible. In order to resolve this infeasibility, the model is updated with additional constraints. If the line power flows from the ACPF solution exceed the original system line power flow constraints, these constraints are added to the model and the DC-OPF SCUC is solved again. This iterative process continues until no line power flows violate the original system constraints. Figure 2.7 shows line power flows on each branch and voltage angles on each bus after iteratively adding line constraints. For the PJM 5 Bus Test System, the final solution was arrived at in a single iteration, and the system results were identical to solving a nodal DC-OPF SCUC. For large systems this iterative approach provides a faster method of attaining a DC-OPF SCUC solution that is more reliable than a simplified DC-OPF SCUC by itself. This has been validated by comparing solve times for a 2383 Bus Test System, as shown in Figure 2.6. This figure shows a box plot of solve times for a single time period DC-OPF SCUC solution when all the line constraints are added (left), compared to when constraints are selectively added (right). We can see that when fewer constraints are added, the model solves consistently faster.

While this may not guarantee in resulting in the globally optimal AC Optimal Power Flow (AC-OPF) SCUC solution and while ACPF solutions for complex systems are not guarenteed to converge, this method can provide a way to make decisions in real world systems in a preferred amount of time. The source data and code for this study is provided in the online repository [31].

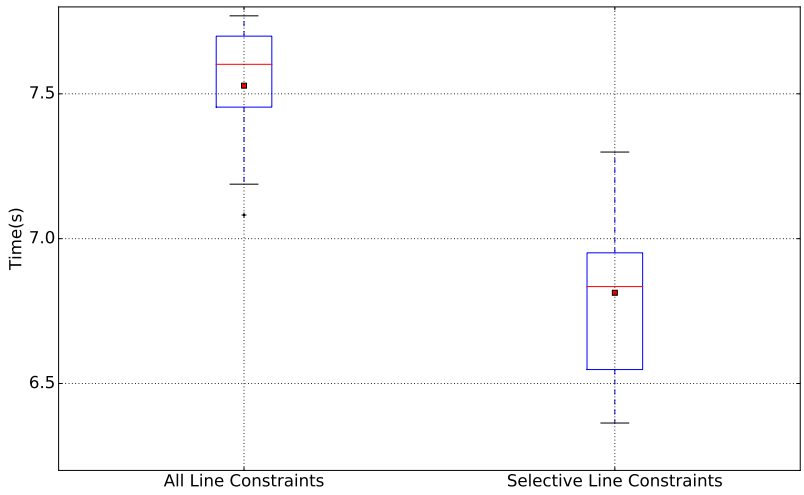

Figure 2.6: Comparing solve times for single time period DC-OPF SCUC when selectively adding line constraints

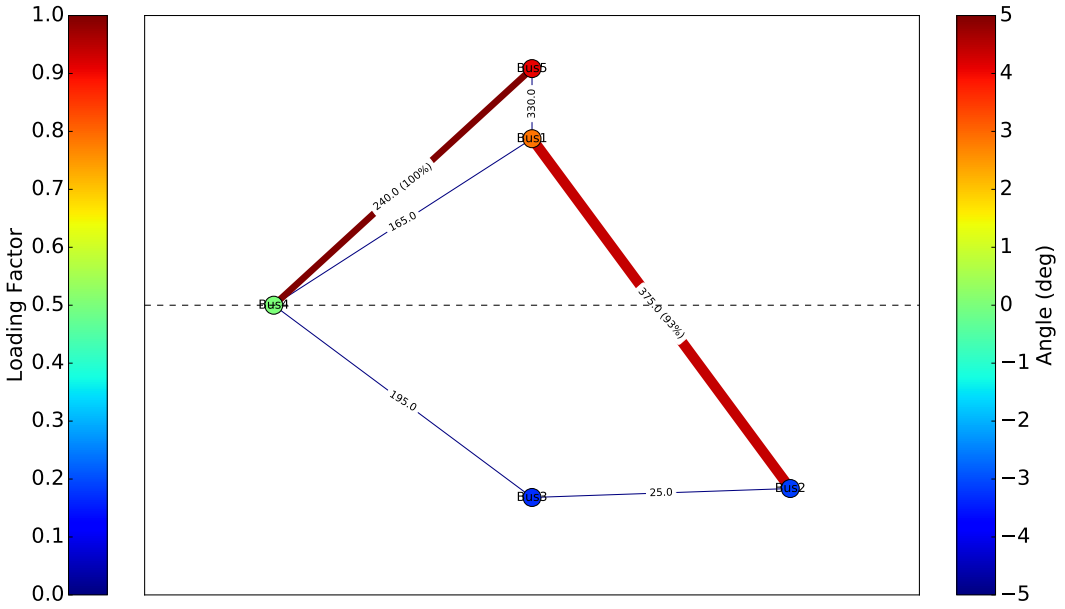

Figure 2.7: Bus voltage angles and line loading of branches in hour 1 for PJM 5 Bus Test System after iteratively adding line constraints

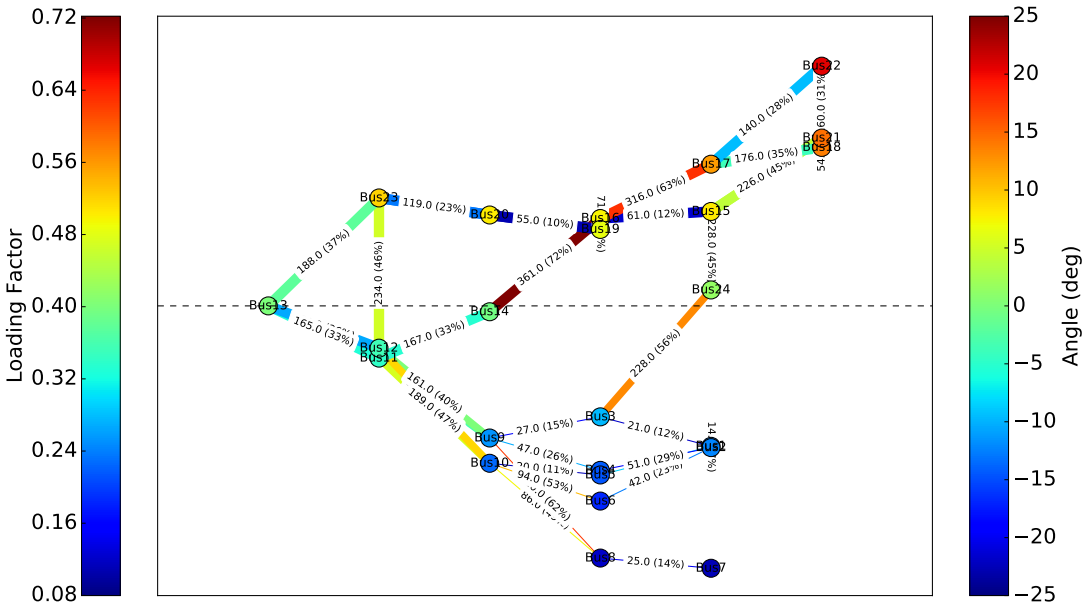

Figure 2.8: Bus voltage angles and line loading of branches for IEEE 24 node system from SCUC DCOPF solution

Additionally, another advantage of this integration is that we can calculate voltage magnitudes and angles for a SCUC commitment solution, to further inform decision making. To demonstrate this, the IEEE 24 node system is built and solved using the SCUC DCOPF formulation, and the generator dispatch values from the unit commitment solution are used to inform the ACPF algorithm. The angles and line power flows from the SCUC DCOPF solution are shown in Figure 2.8. The voltage magnitude and voltage angles for the ACPF solution to the IEEE 24 node system and the angles from the SCUC DCOPF solution are shown in Table 2.1. The root mean square error (RMSE) for the difference between the angles of the SCUC DCOPF solution and the ACPF solution was found to be 3.013 degrees. With the integration of an ACPF solver into PSST, AMES (V4.0) can solve DAM SCUC and RTD SCED problems and provide results for unit commitment and power dispatch of each generator, AC line power flows on each branch, and voltage magnitude and angles at each bus. This information can be invaluable when modeling co-simulation of transmission and distribution systems. Distribution system voltages at each time step can be updated with the voltage solutions from the transmission ACPF.

2.4 Sensitivity Analysis on PTDF formulation compared to $B \times \theta$ formulation

As mentioned earlier, an accurate transmission network model is crucial for modeling a security constrainted optimization model. The transmission network is typically modeled with a DC representation. There are two main ways to model the line power constraints on DC representation of the network. First, the DC power flow constraints can be explicity constructed based directly on the simplication of the power flow equations. The second form of modeling technique is the use of Power Transfer Distribution Factors (PTDFs), also known as shift factors, which can be used to model the line flows in a security constrainted optimization model.

The DC power flow line constraints are typically represented as below, commonly known as the standard $B \times \theta$ formulation.

Table 2.1: Voltage magnitude and voltage angles from ACPF solution compared to voltage angles from SCUC DCOPF solution for the IEEE 24 node test system

BUS_I	V (p.u.)	SCUC DCOPF Angles (deg)	ACPF Angles (deg)
1.0	1.0350	-14.8755	-12.1190
2.0	1.0350	-14.9712	-12.2301
3.0	0.9874	-12.2483	-9.5754
4.0	0.9954	-16.4939	-14.1921
5.0	1.0164	-16.8840	-14.5911
6.0	1.0090	-18.9723	-16.8430
7.0	1.0250	-26.0440	-22.6415
8.0	0.9856	-24.5180	-21.7620
9.0	0.9970	-13.5413	-11.4011
10.0	1.0239	-15.6990	-13.5823
11.0	0.9863	-5.9775	-4.5060
12.0	0.9962	-5.2116	-3.6475
13.0	1.0200	0.0000	0.0000
14.0	0.9861	-2.8156	-0.5059
15.0	1.0140	4.9232	8.1487
16.0	1.0170	4.2782	7.5404
17.0	1.0386	8.5935	12.2273
18.0	1.0500	9.8764	13.6761
19.0	1.0232	2.8891	6.5983
20.0	1.0384	3.6206	7.8441
21.0	1.0500	10.6319	14.4819
22.0	1.0500	16.3379	20.6882
23.0	1.0500	4.7267	9.3157
24.0	0.9771	-1.3409	1.3749

$$w_\ell(k) = S_0 \times B(\ell) \times \left(\theta_{O(\ell)}(k) - \theta_{E(\ell)}(k)\right) \tag{2.1}$$

where $w_\ell(k)$ is the power on line ℓ in hour k, S_0 is the positive base power (in three-phase MVA), $B(\ell)$ is inverse of reactance (pu) on line ℓ $O(\ell)$ is the originating bus for line ℓ $E(\ell)$ is the end bus for line ℓ and $\theta_b(k)$ is the voltage angle (radians) at bus b in hour k. Under this assumption, the reactive power is ignored and the bus voltages are assumed to be 1 pu.

An alternative representation of the DC power flow constraints is based on power transfer distribution factors, also commonly referred to as shift factors. Shift factors are used to determine how the power flow on a line will change if one unit of power is injected into the system

and withdrawn at the reference bus. Shift factors for a system are independent of power generation or load power consumption at points on the system, and strictly depend on the network configuration and network parameters and properties of the system. Hence the shift factors can be calculated, and stored as a matrix with dimensions of the number of branches and the number of buses. With the shift factor matrix defined, the following constraint can be added to unit commitment and economic dispatch problems to represent the security constraints, in place of the standard $B \times \theta$ set of equations.

$$w_\ell(k) = \sum_{b \in Z} PTDF_\ell^b \times P_{net}^b(k) \tag{2.2}$$

where $w_\ell(k)$ is the power on line ℓ in hour k, Z is the set of all buses, $PTDF_\ell^b$ is the power transfer distribution factor for line ℓ and bus b, and $P_{net}^b(k)$ is the net power inject at bus b in hour k. Similar to the previous formulation, the reactive power is ignored and the bus voltages are assumed to be 1 pu.

A shift factor matrix may have high precision to capture the effects on line power changes when power is injected at any bus. However, it is possible that in a real world large system, power injected at a bus may not affect the line power flow on a line that is located far away from the bus in question. Mathematically, when the power flow on a branch is largely unaffected by an injection at a bus, the shift factor that corresponds to that branch bus pair will be a very low value. This shift factor can be neglected to solve a problem faster. However this may lead to inaccuracies. The following senstivitiy analysis aims to characterise these performance of the PTDF formulation with changes to the PTDF shift factor matrix. For the following sensitivity analysis, the RTS-96 Test System [33] is used. The shift factor matrix is stored in a NumPy matrix. For a sensitivity analysis, the precision of the shift factors is changed between runs, leaving all else identical. The simulation was conducted for a single day (July 1st) in the RTS-96 Test System. The MIP gap setting in the solver was set to zero. This was done to ensure that for a given set of input parameters, an accurate solution would be found. Results from the standard $B \times \theta$ model are shown in Table 2.2.

Table 2.2: Standard $B \times \theta$ model build time, model solve time, and objective function

Model Build Time (s)	Model Solve Time (s)	Objective Function ($)
5.45	10.1	949138.5034

Table 2.3: PTDF model build time, model solve time and objective function under different rounding threshold

Threshold	Model Build Time (s)	Model Solve Time (s)	Objective Function ($)
-	8.21	109	949138.7528
1.0e-6	9.77	99	949138.7528
2.5e-6	8.63	100	949138.7528
5.0e-6	7.41	36.1	966892.8801
7.5e-6	7.34	40.6	966892.8801
10.0e-6	7.74	36.6	1058579.039

Table 2.4: PTDF model build time, model solve time and objective function under different rounding precisions

Significant Digits	Model Build Time (s)	Model Solve Time (s)	Objective Function ($)
-	8.21	109	949138.7528
15	9.41	96	949138.9123
14	10.4	60	949139.4777
13	9.51	105	949142.2108
12	8.59	117	949139.2697
11	8.44	114	949134.3732
10	7.54	69	949131.5804
9	8.59	41	949460.0186
8	8.19	27.9	957111.1270
7	8.83	28.7	1024987.529

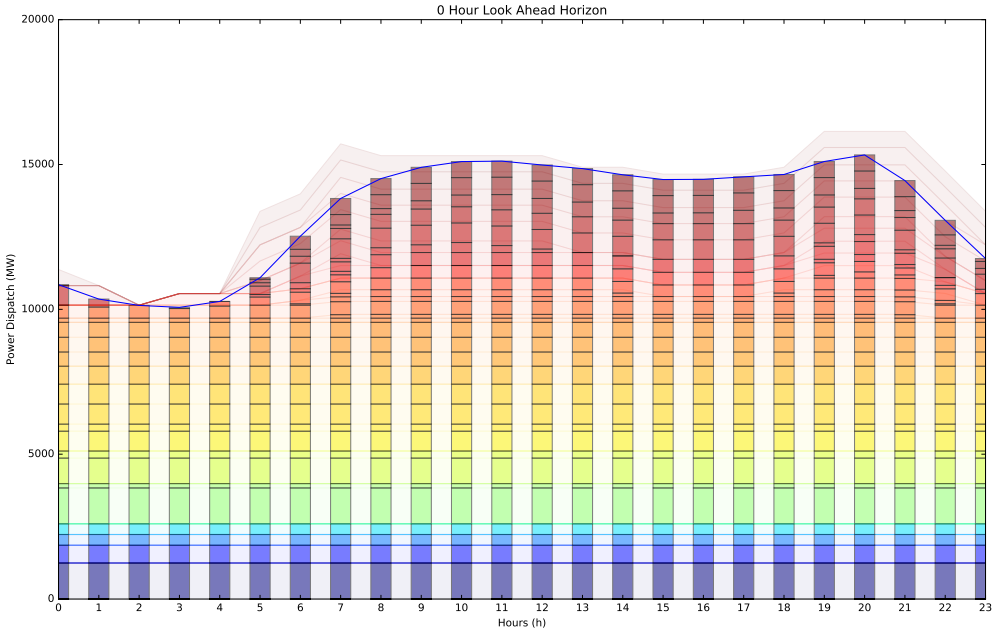

Figure 2.9: Power dispatch and commmited capacity with zero hours look-ahead

From Table 2.3, we can see that on increasing the threshold for shift factors, a large problem can be solved considerably faster. However, this results in a decrease in accuracy of the objective function of an optimization. From Table 2.4 we can see that on decreasing the precision of the shift factors, a speed up can be achieved as well, at the cost of the objective function accuracy decreasing.

2.5 Sensitivity Analysis on Look Ahead Time Horizon for SCUC

A sensitivity analysis on the look ahead time for the unit commitment in the solver model was conducted. Typically, unit commitment operations are solved on day D for 24 hour time periods representing day D+1. This process is repeated on day D+1, solving for the unit commitment decisions on day D+2. Since the optimization does not look ahead to the next day, it is possible that the end state on day D+1 may cause a poor starting condition for day

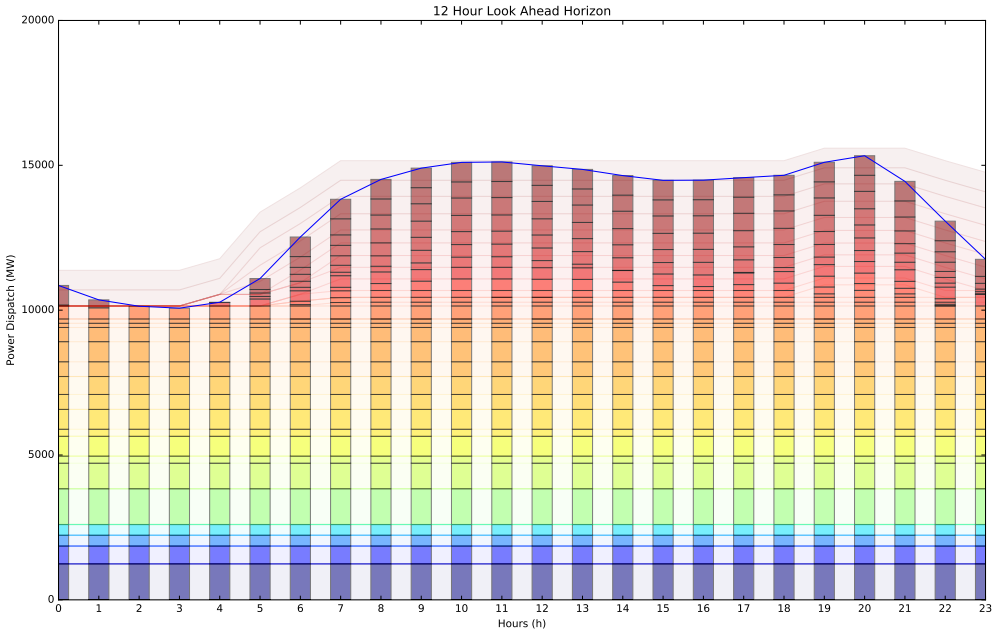

Figure 2.10: Power dispatch and commmited capacity with 12 hours look-ahead

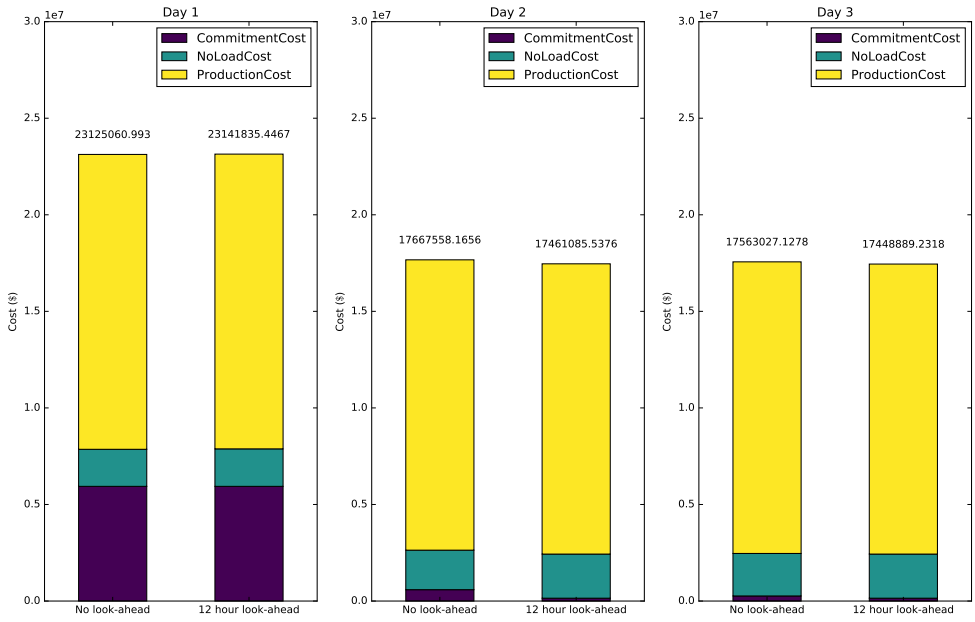

Figure 2.11: Comparison of costs by type and total cost for 3 simulated days

D+2. This poor starting condition could be expensive for the Independent System Operator for operating on day D+2.

This analysis aims to characterise the effect of a look-ahead time horizon of the various costs that contribute to the objective function, namely commitment costs, no-load costs and production costs. The analysis is performed on the 8-Zone Test System based on ISO-NE data described in the previous chapter [1]. A three day simulation was conducted. It can be seen from Figure 2.9 and Figure 2.10 that with a look ahead optimization, additional generators are committed, particularly in the end of the optimization horizon. Since these generators are not dispatched, this increases the no-load cost of the system However, we can see that even though no-load costs increase, commitment costs decrease. Production costs were found to be nearly identical. The total system cost is found to decrease with increase in the look-ahead time period. Figure 2.11 shows the costs for each day comparing a case with no look-ahead horizon

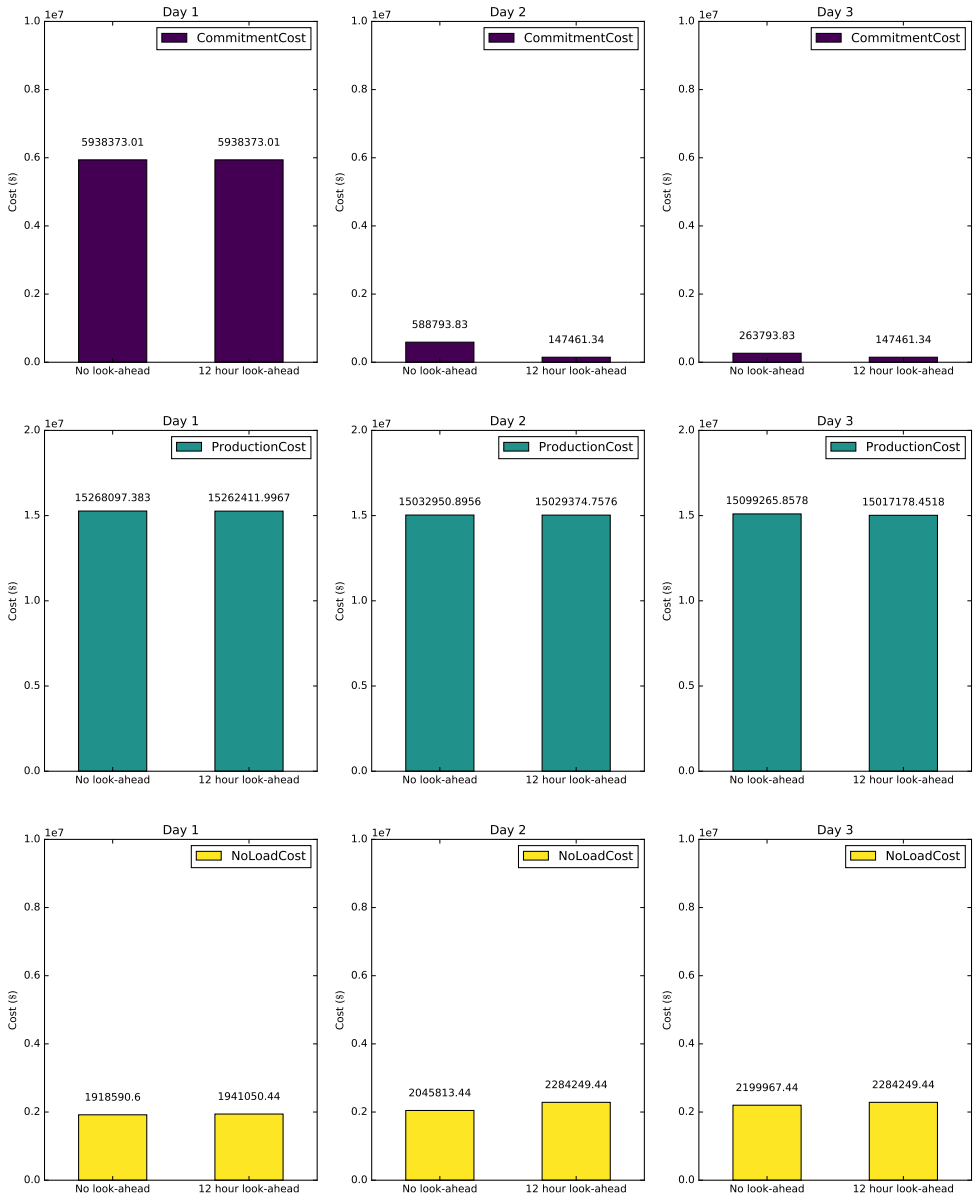

Figure 2.12: Comparison of individual cost type for 3 simulated days

with a 12 hour look-ahead horizon. Figure 2.12 shows the same information split by different cost types, namely commitment costs, production costs, and no-load costs.

2.6 Sensitivity Analysis on Number of Block Segments for SCUC

A sensitivity analysis on number of block segments in the PSST solver was conducted. Generator fuel cost functions curves are typically non convex. As an approximation, they are generally represented as cubic or quadratic functions. The fuel cost function approximation for a thermal plant is close to a quadratic cost function [34], and can be represented as shown in Equation 2.3.

$$C(P_g) = a + b \times P_g + c \times P_g^2 \tag{2.3}$$

where g is the generator unit; P_g is the electrical power output (power generation) of generator unit g; $C(P_g)$ is the operating cost of generator to produce P_g; a, b and c are the fuel cost coefficients of generator g.

For efficiently solving a MILP SCUC, markets allow generators to submit a supply bid that represents their marginal costs. This study shows results comparing solutions using a five-bus test case with a sensitivity analysis performed on the number of blocks in the offer that a GenCo submits into the DAM. From Figure 2.13, we can see that a higher number of segments in a linearized bid can give a more accurate solution for a SCUC, since a greater number of segments will more accurately model a quadratic cost curve function. To understand the impact of the number of segments, a series of tests was conducted with the five-bus test case described in the repository [31] and the nominal root mean square error between formulations with a linearized objective function and a quadratic objective function[2] was compared. With an increase in resolution of the number of segments a higher accuracy is attained, however the time of the solution increases quadratically, as seen in Figure 2.14. For the five-bus test case, a compromise between speed and accuracy is attained at 100 block segments, beyond which there is no significant increase in accuracy.

[2] A quadratic programming formulation was implemented in PSST using SCIP [35] as a solver and the results closely match that of a standard five-bus test case [36]. The solution from the quadratic programming formulation was used as a benchmark for this comparison.

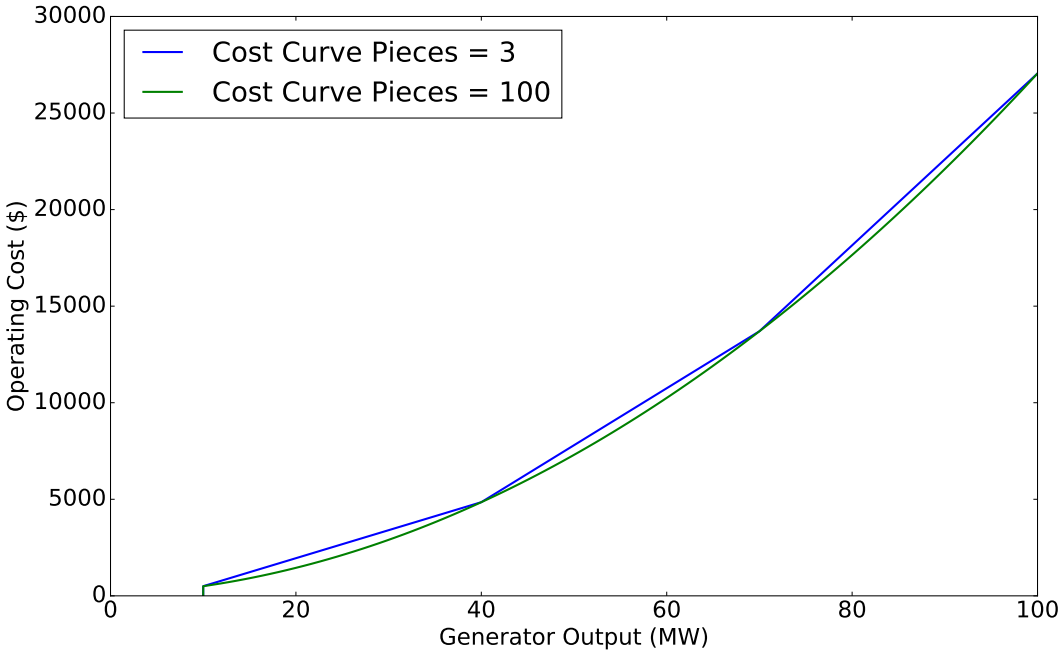

Figure 2.13: Comparison of piecewise cost curve with 3 block segments and 100 block segments

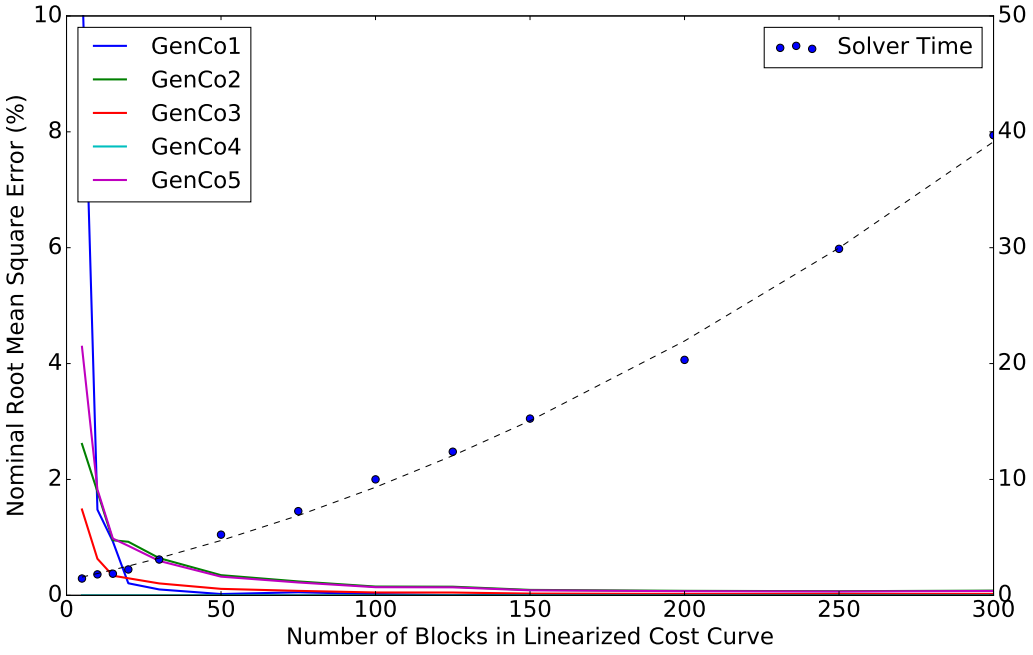

Figure 2.14: Comparison of nominal root mean square error between dispatches from a piecewise linear cost curve formulation and a quadratic cost curve formulation and solution times (seconds) for each corresponding run with increasing block segments of cost curve.

2.7 Verification of Solvers in AMES (V4.0)

Verification of the Pyomo and the PSST solver was carried out in two steps. Firstly, toy test systems were built and solved, and these results were also manually calculated and found to match the experimental results. Secondly, the experimental results from the solver were compared with MATPOWER/PYPOWER and published results. The full set of tests and results can be found in the tests folder of the AMES (V4.0) source code [31]. Some of the tests are described in detail below.

For testing the correctness of the formulation, small test systems were designed. A two node, two generators, two load serving entities and one branch system is considered here. Table 2.5 describes the generator characteristics and Table 2.6 describes the branch characteristics of the system.

Table 2.5: Two Node System Generator Parameters

	GEN BUS	PMAX (MW)	RAMP RATE (MW/hr)
GenCo1	Bus1	200	200
GenCo2	Bus2	500	500

Table 2.6: Two Node System Branch Parameters

	FROM BUS	TO BUS	X (p.u.)	MAX LINE POWER (MW)
Line1	Bus1	Bus2	0.0281	50

It costs GenCo1 10 $/MWhr and GenCo2 14 $/MWhr to produce energy. As described in Table 2.5, GenCo1 is connected to Bus1 and GenCo2 is connected to Bus2. For the first test case described here, load at Bus1 and load at Bus2 are assumed to be 100.0 MW and 300.0 MW respectively. The single time period test system model was built using the standard formulation and solved. It is found that both generators are committed. GenCo1 is dispatched at 150 MW and GenCo2 is dispatched at 250 MW. We can see that since GenCo1 is cheaper, it is dispatched to meet the load at Bus1 and to meet the load partially at Bus2. Since there is a line power limit of 50 MW on the branch between Bus1 and Bus2, and since the total load on the system is greater than GenCo1's capacity, GenCo2 is committed and dispatched to meet to

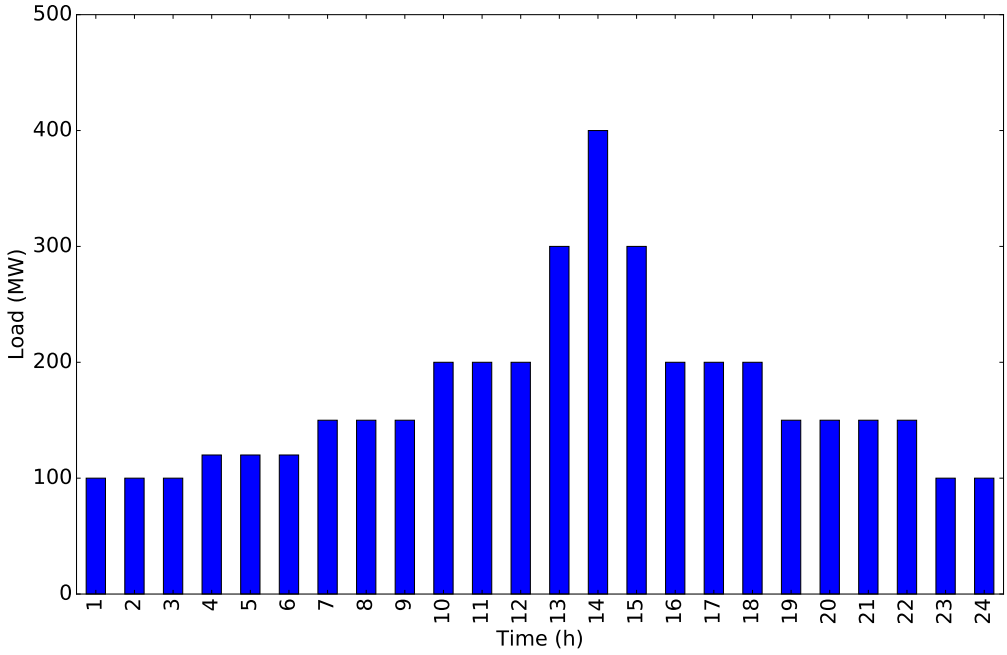

Figure 2.15: Load at Bus2

remaining load at Bus2. The LMPs were also calculated at each bus and were found to be $ 10 and $ 14 on Bus1 and Bus2 respectively. At each bus an additional MW can be served by the generator at that bus and by only the generator at that bus, given the transmission line power limit constraint. This is a verification of the core of the formulation.

Similarly, a test case can be constructed to test the unit commitment formulation. Let us assume that the load at Bus1 is removed, and forecasted load at Bus2 is set to a load profile as shown in Figure 2.15. Also, let GenCo1 start-up, shut-down and no-load cost be defined as shown in Table 2.7.

Table 2.7: Two Node System Generator Parameters

	START UP COST	SHUT DOWN COST	NO LOAD COST
GenCo1	0	0	0
GenCo2	5000	1000	2000

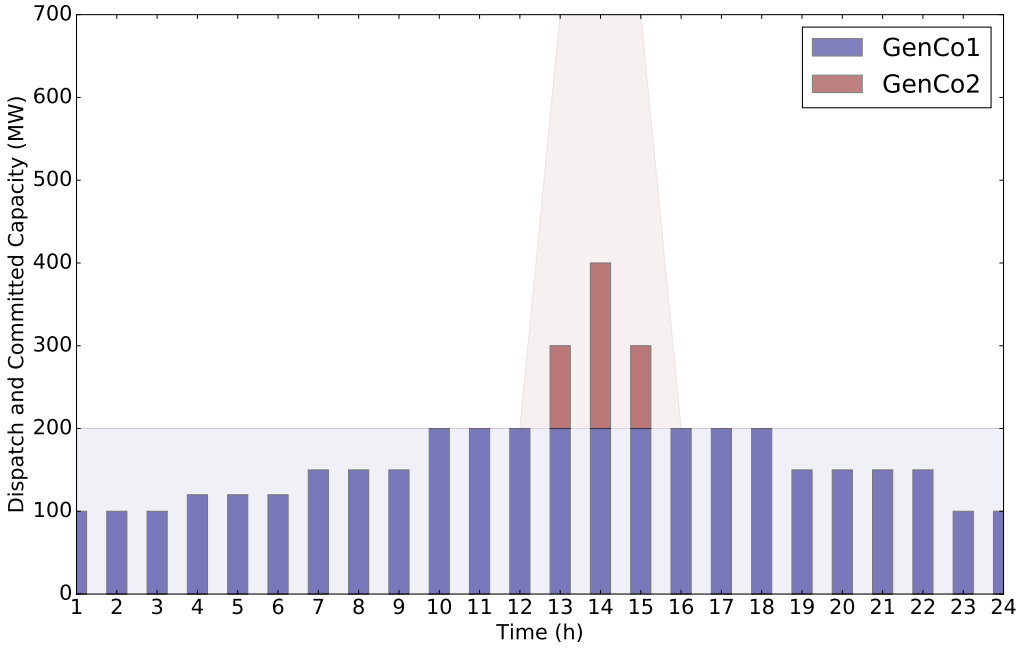

Figure 2.16: Generator dispatch and committed capacity for the two node test system

Since GenCo2 is more expensive, we can expect it to only be committed and dispatched when required. This is seen in Figure 2.16, which shows stacked generator dispatch levels as decided by the SCUC formulation, along with the total committed capacity in the system. The different colors in the stacked plots show the different generators.

To test the minimum up time constraints, we can change the minimum up time of GenCo2 to 5 hours. The results shown in Figure 2.17 are as expected, GenCo2 is turned on for 5 hours but is only dispatched to meet the load for three hours, similar to the previous case.

Similarly, to test the ramp constraints implementation, GenCo2 ramp rate is limited to 50 MW/hr. The model is built and solved, and the results are shown in Figure 2.18. GenCo2 is ramp limited, but GenCo1 is free from ramp constraints. Hence GenCo1 is ramped down while GenCo2 is ramped up to meet the peak load in hour 14.

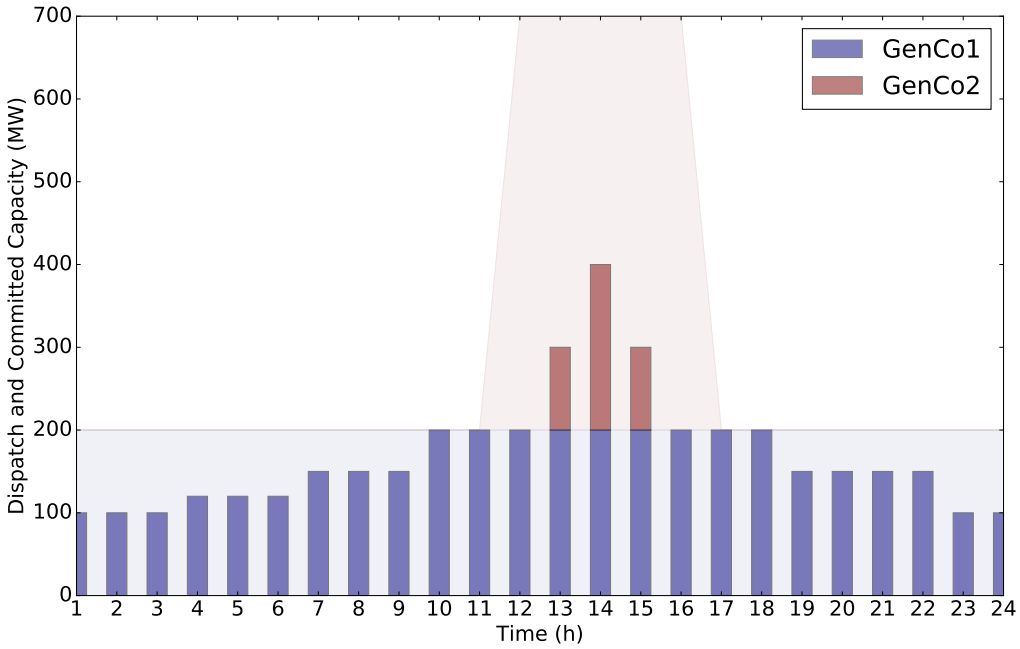

Figure 2.17: Generator dispatch and committed capacity for the two node test system with a 5 hour minimum up time constraint

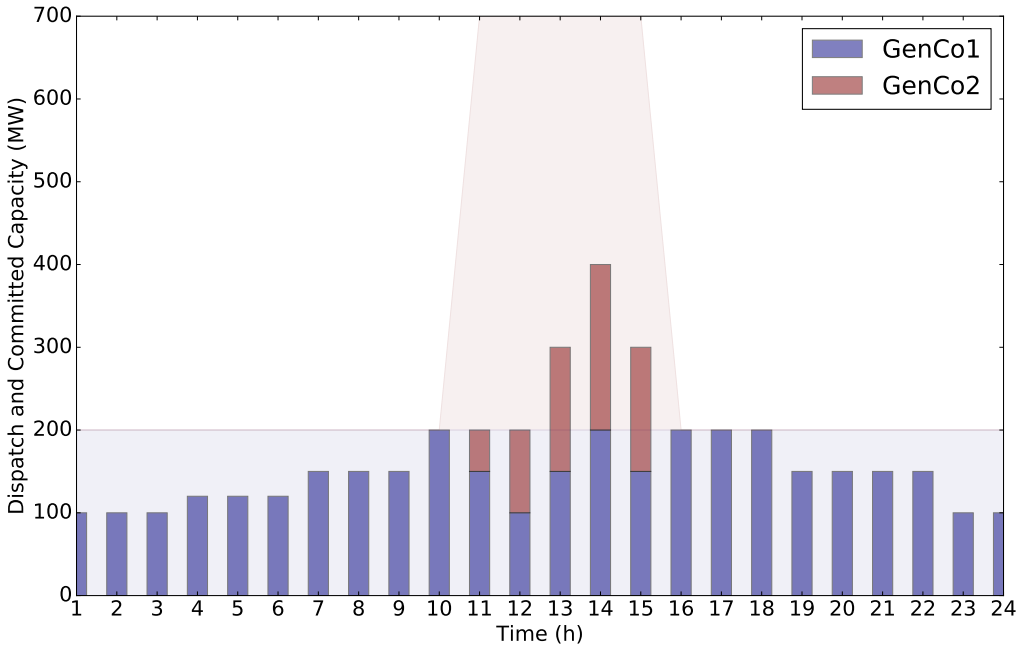

Figure 2.18: Generator dispatch and committed capacity for the two node test system with a 50 MW ramp up and ramp down constraint

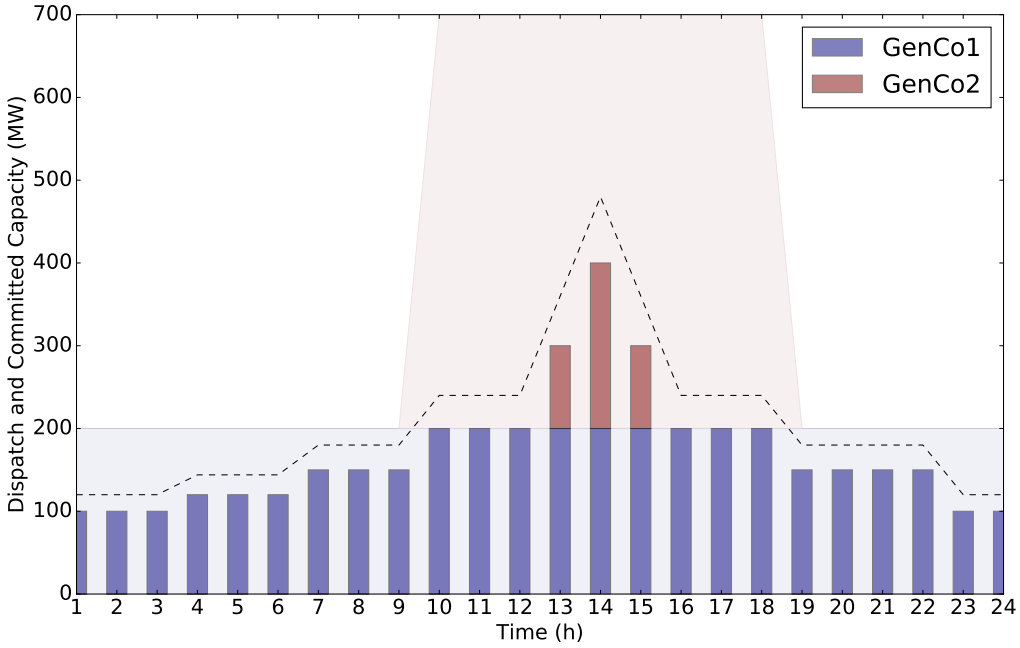

Figure 2.19: Generator dispatch and committed capacity for the two node test system with a system reserve requirement of 20 % of the system load

Figure 2.19 shows results on including a system reserve requirement of 20 % of the system load. Figure 2.20 shows results on including a system reserve requirement of 20 % of the system load along with a 50 MW ramp up and ramp down constraint for GenCo2

These incremental changes to individual parameters have allowed for extensive testing of all constraints in the formulation, including ramp up and down rates, start up and shut down ramp rates, system reserve requirements, startup costs, shutdown costs, and noload costs. The code for all these tests are available in the repository online [31].

In addition to the above tests, the results from 15 standard test cases built using this formulation were compared to results from the DCPF algorithm from MATPOWER/PYPOWER. These results are shown in Table 2.8 and Table 2.9 and show that the solver in AMES (V4.0) performs closely to DCPF and DCOPF algorithm from PYPOWER/MATPOWER respectively. Table 2.10 shows dispatch of all generators and LMPs at all buses for 24 hours from the five-bus

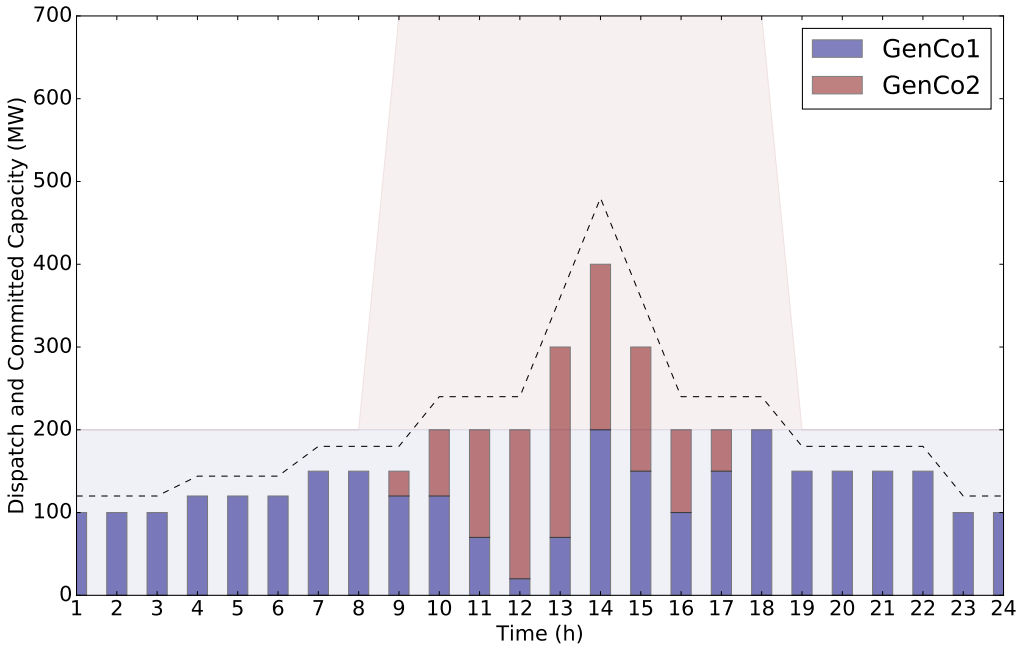

Figure 2.20: Generator dispatch and committed capacity for the two node test system with a system reserve requirement of 20 % of the system load and a 50 MW ramp up and ramp down constraint

Table 2.8: Comparison of DCPF and AMES (V4.0) solver for single time period test system

Case	RMSE Angles (deg)	RMSE Line Power (MW)
case5	1.4486e-15	2.2192e-13
case9	7.3577e-15	5.0051e-14
case6ww	1.2079e-15	1.6274e-14
case14	2.3268e-14	8.9785e-14
case24_ieee_rts	2.2683e-14	2.5062e-13
case30	2.1677e-14	5.2445e-14
case_ieee30	5.7271e-14	1.5363e-13
case39	4.0065e-14	5.8003e-13
case57	1.8475e-14	1.4501e-13
case118	4.8318e-14	3.7028e-13
case300	4.3389e-13	3.0867e-12
case2383wp	8.2231e-11	8.3241e-10
case2746wop	4.0607e-12	2.0301e-11
case2746_wp	2.2408e-12	2.5266e-11

Table 2.9: Comparison of DCOPF and AMES (V4.0) solver for single time period test system

Case	RMSE Power Generation (MW)
case5	2.92631172565e-05
case9	0.0615702573202
case6ww	0.00860337309588
case14	0.0209756821438
case30	0.0226435511815
case_ieee30	0.0440736712184
case39	0.116860594574
case57	0.0933369277266

test case. These results have been compared against results that were published in [36], and the results in both these cases were found identical.

2.8 Concluding Remarks for Chapter 2

This chapter describes implementations of different improvements to AMES (V4.0) and describes the two solver interfaces, explaining the advantages of each interface.

This chapter describes an integration of an ACPF with a SCUC DC-OPF iterative algorithm to improve reliability of solutions for large complex power system problems. In addition, this integration of an ACPF algorithm allows the calculation of voltage magnitudes at each bus,

allowing the accurate integration and modeling of transmission and distribution co-simulation techniques.

This chapter also describes the implementation an alternative formulation (PTDF formulation) and performs a sensitivity analysis to characterise its performance, and contrasts these results to the $B \times \theta$ formulation by performing a comparative study of numerical errors for the two mathematically equivalent formulations. It shows that the PTDF formulation decreases solve times, however results in a lower accuracy of the objective function.

The work in this chapter also demonstrates the effect of a look ahead time period and rolling horizons, and shows that it is beneficial for the ISO to implement such a capability. Finally, this work also describes the effects of number of block segments in the cost curve and shows that accuracy increases by increasing the number of blocks, thereby allowing for improving the accuracy of standard SCUC implementations.

This work has also compared the results from the new version of AMES (V4.0) to the previous version to ensure that no regressions or bugs were introduced in development.

The code to run these studies is released under an open license [31]. Additionally, contributions to a number open source projects (PYPOWER, Pyomo) were made as part of the work for this chapter.

Table 2.10: Dispatch of Generators and LMPs at Buses in five-bus test case reproduced using AMES (V4.0) and PSST

Hour	GenCo1 (MW)	GenCo2 (MW)	GenCo3 (MW)	GenCo4 (MW)	GenCo5 (MW)	Bus1 ($)	Bus2 ($)	Bus3 ($)	Bus4 ($)	Bus5 ($)
1	110.0000	13.8726	332.5342	0.000	443.5932	15.1758	35.5264	31.6707	21.0675	16.2203
2	110.0000	13.4407	269.4121	0.000	437.5372	15.1758	33.9712	30.4101	20.6172	16.1404
3	110.0000	13.1605	227.7024	0.000	433.5372	15.1538	32.9394	29.5697	20.3029	16.0667
4	110.0000	13.0147	206.6580	0.000	431.5173	15.1758	32.4159	29.1495	20.1669	16.0606
5	110.0000	12.8740	185.9916	0.000	429.5344	15.1515	31.9031	28.7293	20.0013	16.0113
6	110.0000	12.9464	196.3265	0.000	430.5271	15.1636	32.1595	28.9394	20.0841	16.036
7	110.0000	13.0143	206.6580	0.000	431.5177	15.1758	32.4159	29.1495	20.1669	16.0606
8	110.0000	13.2998	248.7457	0.000	435.5546	15.1515	33.4584	29.9899	20.4515	16.0911
9	110.0000	14.0130	353.2006	0.000	445.5764	15.1645	36.0475	32.0909	21.2103	16.2364
10	110.0000	14.5841	437.0016	0.000	453.6144	15.1636	38.1214	33.7717	21.8101	16.342
11	110.0000	14.7264	458.0325	0.000	455.6310	15.1879	38.6341	34.1919	21.9758	16.3913
12	110.0000	14.7977	468.3674	0.000	456.6249	15.1895	38.893	34.402	22.0519	16.4061
13	110.0000	14.7257	458.0325	0.000	455.6318	15.1879	38.6341	34.1919	21.9758	16.3913
14	110.0000	14.5836	437.0015	0.000	453.6149	15.1636	38.1214	33.7717	21.8101	16.342
15	110.0000	14.5118	426.6666	0.000	452.6216	15.1557	37.864	33.5616	21.73	16.3212
16	110.0000	14.5111	426.6666	0.000	452.6223	15.1557	37.864	33.5616	21.73	16.3212
17	110.0000	14.7979	468.3674	0.000	456.6247	15.1895	38.893	34.402	22.0519	16.4061
18	0.0000	0.0000	520.0000	108.438	525.1520	14.0522	78.0976	65.9633	32.5939	17.3394
19	107.3477	6.1221	520.0000	0.000	474.1302	15.0722	46.0193	40.156	24.0317	16.6606
20	110.0000	15.0834	510.0807	0.000	460.6260	15.1758	39.933	35.2424	22.3432	16.4464
21	110.0000	15.0101	499.7557	0.000	459.6342	15.1636	39.6767	35.0323	22.2604	16.4218
22	110.0000	14.8690	478.7148	0.000	457.6163	15.1753	39.1555	34.6121	22.1178	16.4061
23	110.0000	14.5114	426.6666	0.000	452.6220	15.1557	37.864	33.5616	21.73	16.3212
24	110.0000	14.0852	363.9125	0.000	446.6023	15.1515	36.3097	32.301	21.277	16.2375

CONCLUSIONS

This thesis delivers on my goal to contribute towards open source test system and test bed development in support of research and engineering in the power system community.

Chapter 1 of this thesis develops an open-source 8-zone test system for teaching, training, and research purposes that is based on ISO New England structural attributes and data. The test system models an ISO-managed wholesale power market populated by a mix of generating companies and load-serving entities that operates through time over an 8-zone AC transmission grid. The modular extensible architecture of the test system permits a wide range of sensitivty studies to be conducted. To the authors knowledge, the open source test system described in chapter 1 is the first release of an empirically-grounded test system that permits systematic study of power market design and performance issues for ISO-NE by means of systematic fast-execution computational experimentation. This test system is published under an open and permissive license to allow other researchers to replicate and expand on this work.

As an illustrative application of the capabilities of the test system developed, a comparative performance study of Stochastic and Deterministic DAM formulations for improved handling of uncertainties in forecasted load scenarios was conducted. Cost-savings outcomes were reported for this comparative study by systematically varying reserve requirement levels for the deterministic formulation. The findings reported in chapter 1 reveal that the expected cost saving arising as a result of a switch from a determinisitc to a stochastic DAM SCUC formulation exhibits a U-shaped dependence on the reserve requirement (RR) for a deterministic SCUC. The key findings in this chapter also reports that for certain RR levels at the nadir of said U shaped curve, cost savings are negative i.e. the deterministic DAM SCUC formulation can outperform the stochastic SCUC formulation.

These findings also demonstrate the ability of simulation studies with small-scale test systems such as the 8-Zone ISO-NE Test System to clarify precise conditions under which different

DAM SCUC formulations can be cost effective. The 8-Zone ISO-NE Test System is implemented via the modular and extensible AMES (V4.0) test bed.

Chapter 2 of this thesis describes the implementation of the various improvements to AMES and showcases the advantages of these improvements in the form of use cases and sensitivity studies. This chapter also describes the thorough validation of the implementation of the formulation in the solvers in AMES.

One of the major improvements in AMES (V4.0) involves the integration of DAM SCUC and RTM SCED formulations into the AMES market modeling framework. The DAM SCUC and RTM SCED formulations were modeled in the open-source optimization modeling language known as Pyomo. Two solvers were implemented in AMES (V4.0) for modeling the DAM SCUC and RTM SCED formulations in Pyomo. Firstly, a direct Pyomo interface was implemented to solve Deterministic and Stochastic SCUC formulations, and to solve Deterministic SCED formulations. Secondly, a PSST (Power System Simulation Toolbox) solver interface was implemented in AMES to solve adaptive dynamic deterministic SCUC and SCED formulations. The PSST solver offers additional flexibility over a direct Pyomo interface and PSST has also been released under an open and permissive license.

Chapter 2 describes use cases of how the new features of AMES (V4.0) can be used to improve modeling of DAM SCUC and RTD SCED formulations. As an illustrative application of the adaptive dynamic formulation, an iterative DC-OPF SCUC and ACPF algorithm was implemented using PSST and this algorithm was validated using a PJM 5 Bus Test System. An iterative algorithm of this nature can improve the reliablity of a SCUC DC-OPF formulation implemented by an ISO. Another advantage of an integration of an ACPF with a SCUC DC-OPF is that this approach includes the voltage magnitudes at each bus on the power system into the SCUC and SCED solutions. This can be extremely valuable when modeling the co-simulation of transmission and distribution systems.

The second use case is presented in chapter 2 in the form of a sensitivity analysis on an alternate formulation of the OPF problem. This analysis characterises the performance of the Power Transfer Distribution Factors (PTDF) formulation, and compares these results to the $B \times \theta$ formulation. A sensitivity analysis of the solution time and the objective function is

performed by varying the precision and threshold of values in the shift factor matrix. This analysis illustrates a method for decreasing solve times for large systems at a cost to objective function accuracy.

Two additional sensitivity analyses were performed on the SCUC formulation. A sensitivity analysis on the look ahead time for the unit commitment in the solver was conducted using the 8-Zone Test System based on ISO-NE data and this analysis compares commitment cost, no load cost and production cost. A sensitivity analysis was also conducted on the effects of increasing the number of bid segments in the cost curve for generators. This study was performed using the PJM 5 Bus Test System, and demonstrates a clear way to improve the accuracy of the DAM SCUC formulation.

Lastly, chapter 2 presents a detailed description of the steps taken to validate the solver in AMES (V4.0). This validation was performed by designing a two node test system for testing single time period DC-OPF models and for testing multi-time period DC-OPF SCUC models. A detailed validation of individual constraints including minimum up time, minimum down time, ramp up rates, ramp down rates, system reserve constraints, transmission line congestion, and LMP, production cost, no-load cost and commitment cost calcuation was carried out and the results were confirmed to be correct. Additionally, 15 MATPOWER test cases were built using the SCUC DCOPF formulation and solved, and the comparison to a DC Power Flow algorithm was reported. This comparison shows the the accuracy of the SCUC DCOPF solution by comparing line power on the branches and voltage angles on the buses against a DCPF algorithm.

All test cases and source code for running the studies described in this thesis have been published under open and permissive licenses to allow reproduciblity and to aid future researchers to develop, build and expand on this work.

Bibliography

[1] D. Krishnamurthy, W. Li, and L. Tesfatsion, "An 8-zone Test System Based on ISO New England Data: Development and Application," *IEEE Transactions on Power Systems*, vol. 31, no. 1, pp. 234–246, Jan 2016.

[2] AMES Wholesale Power Market Test Bed Homepage. [Online]. Available: http://www.econ.iastate.edu/tesfatsi/AMESMarketHome.htm

[3] D. Krishnamurthy, "psst - an open source power system simulation toolbox in python," *North American Power Symposium (NAPS)*, Sep 2016.

[4] DOE Office of Management, "Technology Readiness Assessment Guide," Department of Energy, DOE G 413.3-4A, Tech. Rep., September 2011. [Online]. Available: https://www.directives.doe.gov/directives-documents/400-series/0413.3-EGuide-04a

[5] Q. Wang, J. McCalley, T. Zheng, and E. Litvinov, "A computational strategy to solve preventive risk-based security-constrained OPF," *IEEE Trans. on Power Syst.*, vol. 28, no. 2, pp. 1666–1675, May 2013.

[6] "Power System Test Case Archive," University of Washington. [Online]. Available: http://www.ee.washington.edu/research/pstca/

[7] C. Grigg and et al., "The IEEE reliability test system-1996: A report prepared by the reliability test system task force of the application of probability methods subcommittee," *IEEE Trans. on Power Syst.*, vol. 14, no. 3, pp. 1010–1020, Aug 1999.

[8] Q. Binh Dam, A. P. S. Meliopoulos, G. Heydt, and A. Bose, "A breaker-oriented, three-phase IEEE 24-substation test system," *IEEE Trans. on Power Syst.*, vol. 25, no. 1, pp. 59–67, Feb 2010.

[9] A. K. Singh and B. C. Pal, "Report on the 68-bus 16-machine 5-area system, version 3.3," IEEE PES Task Force on Benchmark Systems for Stability Controls, Tech. Rep., December 2013.

[10] R. Zimmerman, C. Murillo-Sánchez, and R. Thomas, "MATPOWER: Steady-state operations, planning and analysis tools for power systems research and education," *IEEE Trans. on Power Syst.*, vol. 26, no. 1, pp. 12–19, February 2011.

[11] J. Lally, "Financial transmission rights: Auction example," ISO New England M-06, Tech. Rep., January 2002.

[12] J. Sun and L. Tesfatsion, "Dynamic testing of wholesale power market designs: An open-source agent-based framework," *Computational Economics*, vol. 30, pp. 291–327, 2007.

[13] H. Li and L. Tesfatsion, "Development of open source software for power market research: The AMES test bed," *Journal of Energy Markets*, vol. 2, no. 2, pp. 111–128, 2009.

[14] F. Li and R. Bo, "Small test systems for power system economic studies," in *Power and Energy Society Gen. Meet., IEEE*, July 2010, pp. 1–4.

[15] FERC, "RTO unit commitment test system," Federal Energy Regulatory Commission, Tech. Rep., July 2012.

[16] J. Price and J. Goodin, "Reduced network modeling of WECC as a market design prototype," in *Power and Energy Society Gen. Meet., IEEE*, July 2011.

[17] J. Morales, A. Conejo, and J. Pérez-Ruiz, "Economic valuation of reserves in power systems with high penetration of wind power," *IEEE Trans. on Power Syst.*, vol. 24, no. 2, pp. 900–910, May 2009.

[18] A. Papavasiliou, S. Oren, and R. O'Neill, "Reserve requirements for wind power integration: A scenario-based stochastic programming framework," *IEEE Trans. on Power Syst.*, vol. 26, no. 4, pp. 2197–2206, Nov 2011.

[19] M. Vrakopoulou, K. Margellos, J. Lygeros, and G. Andersson, "A probabilistic framework for reserve scheduling and N-1 security assessment of systems with high wind power penetration," *IEEE Trans. on Power Syst.*, vol. 28, no. 4, pp. 3885–3896, Nov 2013.

[20] D. Krishnamurthy. 8-Zone ISO-NE Test System: Code and data repository. [Online]. Available: https://bitbucket.org/kdheepak/eightbustestbedrepo

[21] FERC, "Notice of white paper," U.S. Federal Energy Regulatory Commission, April 2003.

[22] ISO-NE Homepage. [Online]. Available: http://www.iso-ne.com/

[23] A. R. Bergen and V. Vittal, *Power systems analysis.* Prentice Hall, 1999.

[24] D. Deno and L. Zaffanella, "Transmission line reference book 345 kv and above," 1982.

[25] 2013-14 ISO-NE Regional Profile. [Online]. Available: http://www.iso-ne.com/nwsiss/grid_mkts/key_facts/final_regional_profile_2014.pdf

[26] U.S. Energy Information Administration (EIA) Homepage. [Online]. Available: http://www.eia.gov/

[27] ISO New England energy offer data. [Online]. Available: http://www.iso-ne.com/isoexpress/web/reports/pricing/-/tree/day-ahead-energy-offer-data

[28] MISO Regulation Mileage Year One Analysis. [Online]. Available: https://www.misoenergy.org/Library/Repository/Tariff/FERC%20Filings/2014-02-18%20Docket%20No.%20ER12-1664-000,%20et%20al.pdf

[29] M. Carrion and J. Arroyo, "A computationally efficient mixed-integer linear formulation for the thermal unit commitment problem," *IEEE Trans. on Power Syst.*, vol. 21, no. 3, pp. 1371–1378, Aug 2006.

[30] H. Heitsch and W. Römisch, "Scenario reduction algorithms in stochastic programming," *Comp. Opt. Applic.*, vol. 24, no. 2-3, pp. 187–206, 2003.

[31] D. Krishnamurthy. Data and code repository. [Online]. Available: http://kdheepak.com/AMES-v4.0/

[32] W. E. Hart, C. Laird, J.-P. Watson, and D. L. Woodruff, *Pyomo - Optimization Modeling in Python*. Springer Publishing Company, Incorporated, 2012.

[33] C. Grigg, P. Wong, P. Albrecht, R. Allan, M. Bhavaraju, R. Billinton, Q. Chen, C. Fong, S. Haddad, S. Kuruganty, W. Li, R. Mukerji, D. Patton, N. Rau, D. Reppen, A. Schneider, M. Shahidehpour, and C. Singh, "The ieee reliability test system-1996. a report prepared by the reliability test system task force of the application of probability methods subcommittee," *IEEE Transactions on Power Systems*, vol. 14, no. 3, pp. 1010–1020, Aug 1999.

[34] D. Ogilvie, "SYSC-505 Power System Economic Dispatch," 2010.

[35] T. Achterberg, "SCIP: Solving constraint integer programs," *Mathematical Programming Computation*, vol. 1, no. 1, pp. 1–41, 2009, http://mpc.zib.de/index.php/MPC/article/view/4.

[36] H. Li, J. Sun, and L. S. Tesfatsion, "Separation and Volatility of Locational Marginal Prices in Restructured Wholesale Power Markets," Iowa State University, Department of Economics, Staff General Research Papers 13075, Jun. 2009. [Online]. Available: https://ideas.repec.org/p/isu/genres/13075.html